

AD-A095 705

IOWA STATE UNIV AMES ENGINEERING RESEARCH INST
AERODYNAMICS OF ADVANCED AXIAL-FLOW TURBOMACHINERY.(U)
NOV 80 G K SEROVY, P KAVANAGH, T H OKIISHI
ISU-ERI-AMES-81104

F/6 20/4

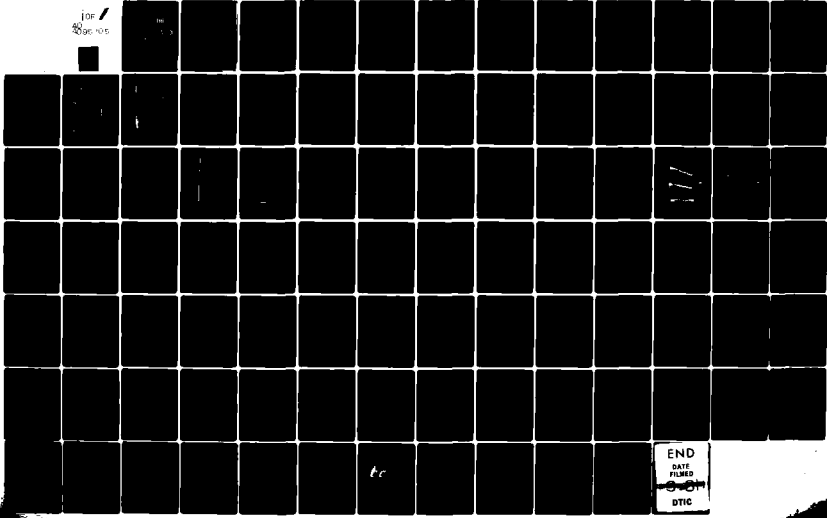
F49620-79-C-0002

AFOSR-TR-81-0109

NL

UNCLASSIFIED

1 OF 1
000000



END
DATE
FILMED
DTIC

Yes

AD 79617
79

George K. Serovy
Patrick Kavanagh
Theodore H. Okishi
November 1980

12

AD A096805

LEVEL III

DTIC
ELECTE
S MAR 0 2 1981 D
E

AERODYNAMICS OF ADVANCED AXIAL-FLOW TURBOMACHINERY

Final Report
1 October 1978 - 30 September 1980

TURBOMACHINERY
COMPONENTS RESEARCH PROGRAM

DDC FILE COPY

APPROVED FOR PUBLIC RELEASE; DISTRIBUTION UNLIMITED

ISU-ERI-Ames-81104
TCRL-17
Projects 1392-1395

ENGINEERING RESEARCH INSTITUTE
IOWA STATE UNIVERSITY
AMES, IOWA 50010 USA

81 2 27 073

**Qualified requestors may obtain additional copies from the
Defense Documentation Center; all others should apply
to the National Technical Information Service.**

CONDITIONS OF REPRODUCTION

**Reproduction, translation, publication, use and disposal in whole
or in part by or for the United States Government is permitted.**

**ENGINEERING
RESEARCH**
**ENGINEERING
RESEARCH**
**ENGINEERING
RESEARCH**
**ENGINEERING
RESEARCH**
**ENGINEERING
RESEARCH**

Final Report
1 October 1978 - 30 September 1980

**AERODYNAMICS OF ADVANCED
AXIAL-FLOW TURBOMACHINERY**

George K. Serovy
Patrick Kavanagh
Theodore H. Oklishi

November 1980

AIR FORCE OFFICE OF SCIENTIFIC RESEARCH (AFSC)
NOTICE OF CONTRACTING TO GO
This technical report has been reviewed and is
approved for distribution under IAW AR 190-12 (7b).
Distribution is unlimited.
A. D. BLOSE
Technical Information Officer

ISU-ERI-Ames-81104
TCRL-17
Projects 1392-1395

**TURBOMACHINERY COMPONENTS RESEARCH LABORATORY
DEPARTMENT OF MECHANICAL ENGINEERING
ENGINEERING RESEARCH INSTITUTE
IOWA STATE UNIVERSITY AMES, IOWA 50011**

Unclassified

14 101-6-111-111
T011-11

SECURITY CLASSIFICATION OF THIS PAGE (When Data Entered)

REPORT DOCUMENTATION PAGE		READ INSTRUCTIONS BEFORE COMPLETING FORM
1. REPORT NUMBER AFOSR-TR--8--0-09	2. GOVT ACCESSION NO. AD-AC95705	3. RECIPIENT'S CATALOG NUMBER
4. TITLE (and Subtitle) AERODYNAMICS OF ADVANCED AXIAL-FLOW TURBOMACHINERY		5. TYPE OF REPORT & PERIOD COVERED Final Report. 1 Oct 1978 - 30 Sep 1980
		6. PERFORMING ORG. REPORT NUMBER TCRL-17
7. AUTHOR(s) George K. Serovy, Patrick Kavanagh and Theodore H. Okiishi		8. CONTRACT OR GRANT NUMBER(s) F49620-79-C-0002
9. PERFORMING ORGANIZATION NAME AND ADDRESS Engineering Research Institute Iowa State University Ames, Iowa 50011		10. PROGRAM ELEMENT, PROJECT, TASK AREA & WORK UNIT NUMBERS G1103F 2 307/A1
11. CONTROLLING OFFICE NAME AND ADDRESS Air Force Office of Scientific Research Directorate of Aerospace Sciences (AFOSR/NA) Bldg. 410, Bolling Air Force Base, Wash., D.C.		12. REPORT DATE 30 November 1980
14. MONITORING AGENCY NAME & ADDRESS (if different from Controlling Office)		13. NUMBER OF PAGES 81
		15. SECURITY CLASS. (of this report) Unclassified
		15a. DECLASSIFICATION DOWNGRADING SCHEDULE
16. DISTRIBUTION STATEMENT (of this Report) Approved for Public Release; Distribution Unlimited		
17. DISTRIBUTION STATEMENT (of the abstract entered in Block 20, if different from Report)		
18. SUPPLEMENTARY NOTES		
19. KEY WORDS (Continue on reverse side if necessary and identify by block number) axial-flow turbomachinery cascade flow axial-flow compressor computational fluid mechanics axial-flow turbine periodically unsteady flow turbomachine flow measurement turbomachinery research facilities		
20. ABSTRACT (Continue on reverse side if necessary and identify by block number) A multi-task research program on aerodynamic problems in advanced axial-flow turbomachine configurations was carried out at Iowa State University. The elements of this program were intended to contribute directly to the improvement of compressor, fan, and turbine design methods. Experimental efforts in intra-passage flow pattern measurements, unsteady blade row interaction, and control of secondary flow are included, along with computational work on inviscid-viscous interaction blade passage flow techniques. This		

DD FORM 1473 1 JAN 73

Unclassified
SECURITY CLASSIFICATION OF THIS PAGE (When Data Entered)

Unclassified

SECURITY CLASSIFICATION OF THIS PAGE(When Data Entered)

20. (cont'd)

cont.

Final Report summarizes the results of this program and indicates directions which might be taken in following up these results in future work.

In a separate task a study was made of existing turbomachinery research programs and facilities in universities located in the United States. Some potentially significant research topics are discussed which might be successfully attacked in the university atmosphere.



Accession For	
NTIS GRA&I	<input checked="" type="checkbox"/>
DTIC TAB	<input type="checkbox"/>
Unannounced	<input type="checkbox"/>
Justification	
By	
Distribution/	
Availability Codes	
Dist	Avail and/or Special
A	

Unclassified

SECURITY CLASSIFICATION OF THIS PAGE(When Data Entered)

TABLE OF CONTENTS

SECTION	<u>PAGE</u>
I. INTRODUCTION	1
II. RESULTS OF THE RESEARCH PROGRAM	3
1. Task I: Analytical and Experimental Investigation of In-Passage Flow in a Constant Mean Radius Rectangular Cross-Section Passage Representative of Passages in Turbomachinery	4
2. Task II: Evaluation and Management of Unsteady Flow Effects in Axial-Flow Compressors	29
3. Task III: Development of a Design-System Oriented Deviation Angle Prediction Equation for Advanced Compressor and Fan Configurations	43
4. Task IV: Experimental Study of Merits of Specific Flow Path Geometry Changes in Controlling Secondary Flows in Axial-Flow Compressors	52
5. Task V: Definition of Experimental Programs and Facilities Appropriate for University Turbomachinery Research Programs	61
III. PUBLICATIONS	65
IV. PROGRAM PERSONNEL	68
V. INTERACTION WITH FEDERAL AGENCIES AND INDUSTRY	69
VI. DISCOVERIES, INVENTIONS, AND SCIENTIFIC APPLICATIONS	73
VII. CONCLUDING REMARKS	74
SYMBOLS AND NOTATION	76
REFERENCES	78
APPENDIX A: EXPERIMENTAL DATA TABULATION FOR PASSAGE TEST RIG, TASK I	81

SECTION I
INTRODUCTION

During the past twenty years a coordinated program of research on problems related to the fluid dynamics of axial-flow turbomachinery has been developed at Iowa State University in the Turbomachinery Components Research Laboratory. Numerous projects funded by the National Aeronautics and Space Administration (NASA), the United States Air Force Office of Scientific Research (USAF/AFOSR), the United States Air Force Aero Propulsion Laboratory (USAF/AFAPL), the Naval Air Systems Command, and other government and industrial organizations have been completed. Beginning 1 October 1978, the Iowa State University Department of Mechanical Engineering faculty involved with turbomachinery research were funded through AFOSR Contract F49620-79-C-0002 to develop a multi-task program concentrating on problems in the aerodynamics of advanced axial-flow compressors, fans, and turbines. Five projects were scheduled during the initial two-year contract period.

- Task I: Analytical and Experimental Investigation of Intra-passage Flow in a Constant Mean Radius Rectangular Cross-Section Passage Representative of Passages in Turbomachinery
- Task II: Evaluation and Management of Unsteady Flow Effects in Axial-Flow Compressors
- Task III: Development of a Design-System Oriented Deviation Angle Prediction Equation for Advanced Compressor and Fan Configurations

Task IV: Experimental Study of Merits of Specific Flow Path
Geometry Changes in Controlling Secondary Flows in
Axial-Flow Compressors

Task V: Definition of Experimental Programs and Facilities
Appropriate for University Turbomachinery Research
Programs

Section II of this report reviews the progress made in reaching
the objectives in each Task.

SECTION II

RESULTS OF THE RESEARCH PROGRAM

Each of the five projects in the contract program is discussed in this section. Task I originated in internally-supported work at Iowa State University and is based on earlier analyses carried out with support from the Pratt & Whitney Group of the United Technologies Corporation. Task II is a continuation of research funded by AFOSR since 1975. Task III continues computation and analysis initiated in 1974 with funding from NASA and extended under an AFOSR grant in 1978. Task IV evolved from discussions with Dr. Arthur J. Wennerstrom of AFAPL, and is intended to result in fundamental design data that will be usable in future high-efficiency multistage axial-flow compressor development. Task V is an independent study of the current capabilities of university turbomachine research groups in the United States, and of project areas in which these groups can make significant technical contributions.

1. TASK I: EXPERIMENTAL AND ANALYTICAL INVESTIGATION OF INTRAPASSAGE FLOW IN A CONSTANT MEAN RADIUS RECTANGULAR CROSS-SECTION PASSAGE REPRESENTATIVE OF PASSAGES IN TURBOMACHINERY

1.1. Introduction

The application of two-dimensional or blade-element design systems for turbomachinery cascades is often subject to failure in cases where large secondary flows result from the interaction of endwall boundary layers with the remainder of the flow field. This is especially true in low aspect ratio geometries where the influence of the endwalls may be felt throughout the entire flow passage. It has been recognized for some time that extensive additional information is required to help supplement practical cascade design systems, with, ultimately, three-dimensional flow analyses forming the basis for such design systems. For this reason, a detailed investigation of intrapassage flow in a large-scale, curved rectangular cross section passage representative of turbomachinery passages was undertaken. The experimental results thus obtained may provide further knowledge of the complex internal flow structure involved and may also be used in evaluating and checking theoretical analyses as they are developed in future work.

1.2. Experimental Facility and Passage Test Rig

In the subject curved passage, significant secondary flow can occur without additional complications of cascade leading and trailing edge effects and tip clearance flows. Also with low-speed, incompressible flow testing the essential details of the three-dimensional flow field are present. In the present investigation, the test passage consists of

a 90-deg. bend of constant mean radius followed by a straight discharge section as shown in the schematic diagram in Fig. 1. The actual test passage, inlet and discharge sections, and associated instrumentation are shown in the photographs in Figs. 2, 3 and 4.

Air flow to the test rig is supplied by the Turbomachinery Low-Speed Flow Loop which consists of a large centrifugal blower with design flow rate of 20,000 cfm at 20 inches of water head rise, variable-speed drive and motor, a piping system of 30-inch diameter pipe including metering section and supply header, and a large diameter plenum discharge section. Contained in the plenum is a series of screens and a honeycomb to ensure satisfactory flow uniformity and turbulence level. The flow loop is operated open-circuit for the present testing with flow exhausting from the test rig to atmosphere.

The test section proper consists of the 90-deg. bend and discharge passage as formed by the upper and lower endwalls, and by the inner (suction) and outer (pressure) sidewalls. As can be seen in Fig. 2, the upper endwall, which was fabricated from 19-mm thick aluminum tooling plate, contains 12 traverse slots across the flow passage at uniformly spaced stations in the flow through the bend and straight discharge sections. Brass tooling bar stock (9.525 mm by 19.050 mm) was used for the traverse slide bars in the aluminum endwall. These slide bars, which were precision-fitted in the endwall to produce a smooth inner wall for the passage, were used to carry a five-hole directional pressure probe and a static tap fixture for mapping out the details of the flow in each traverse plane. The slide bars, each actually composed of two

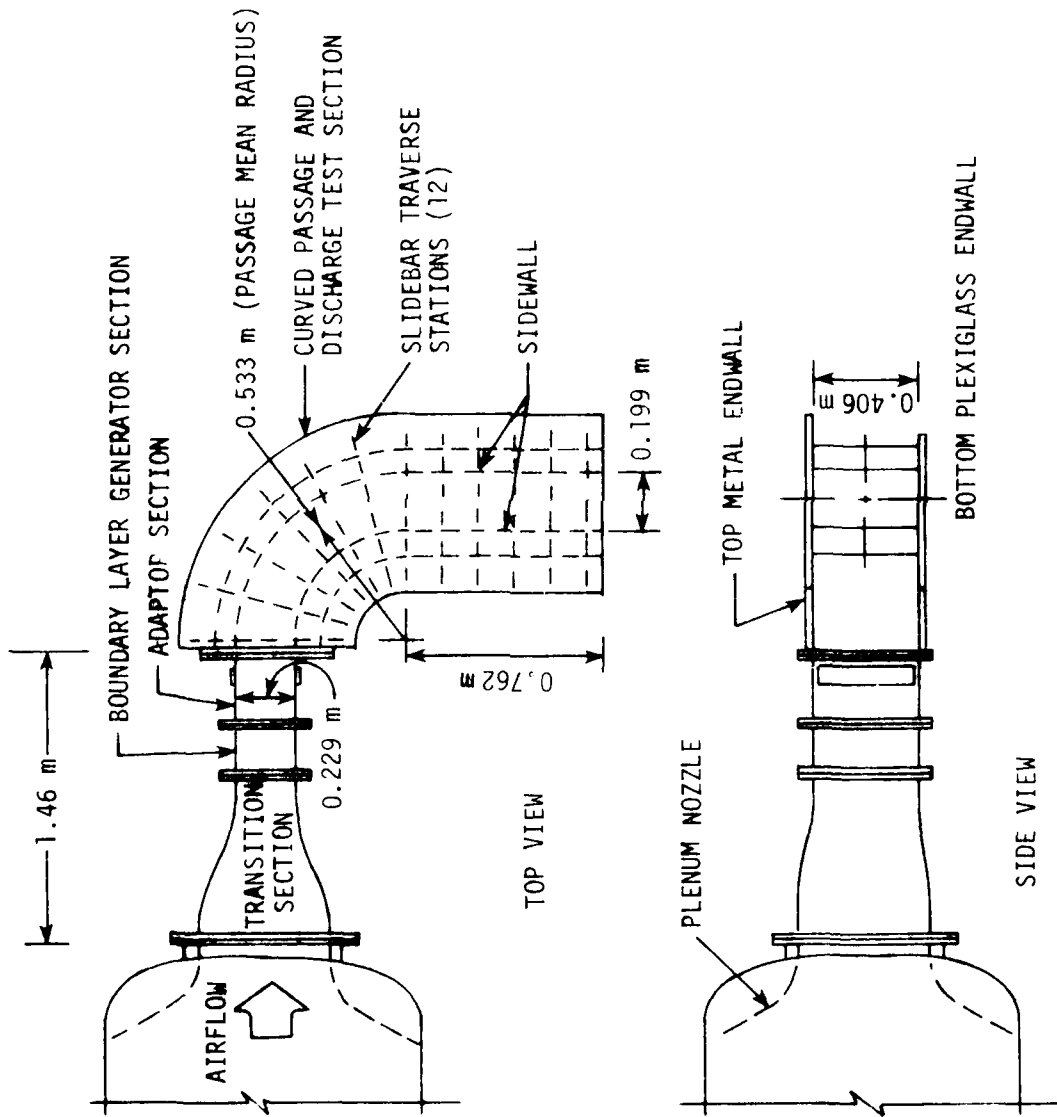


Figure 1. Schematic diagram of passage test rig, Task I.



Figure 2. Plan view of passage test rig installed on plenum in laboratory, Task I.

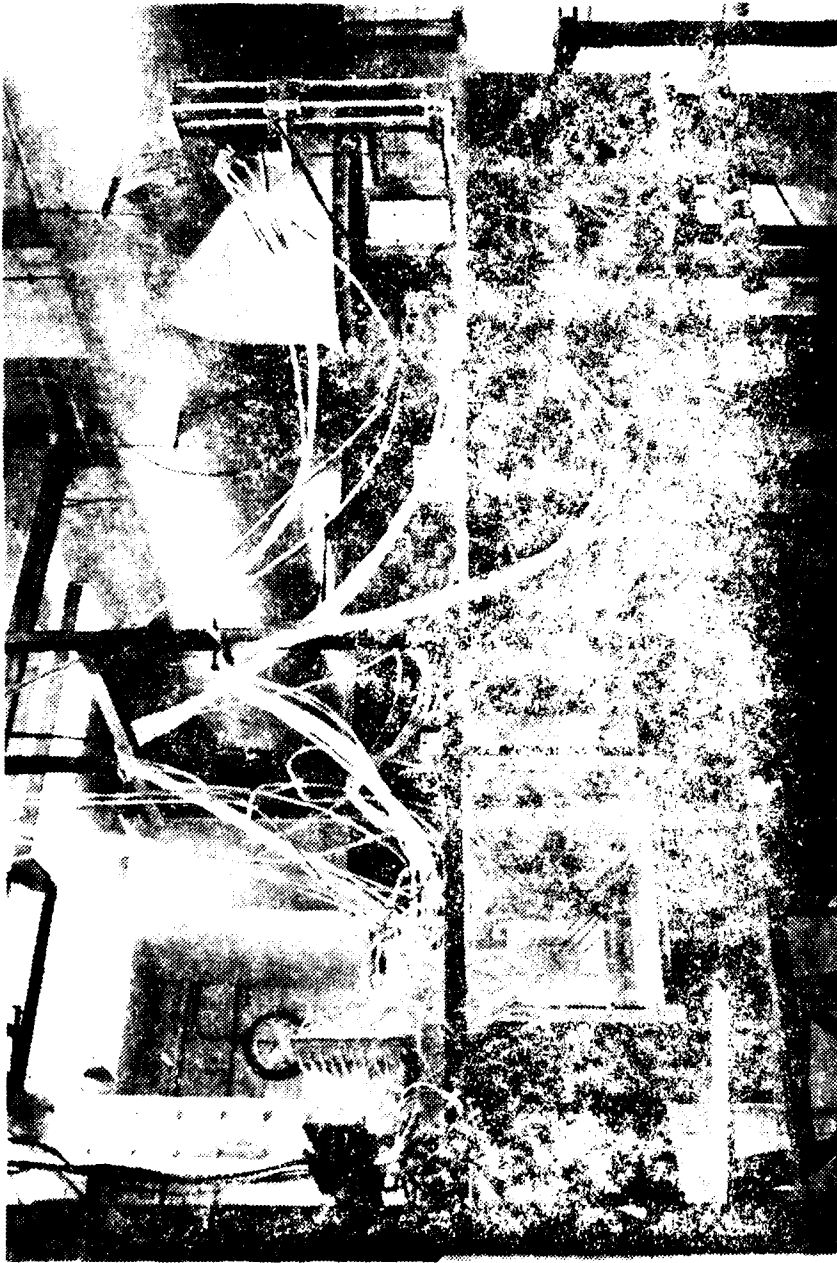


Figure 3. Side view of passage test rig installed on plenum in laboratory as seen from suction side of bend, Task I.

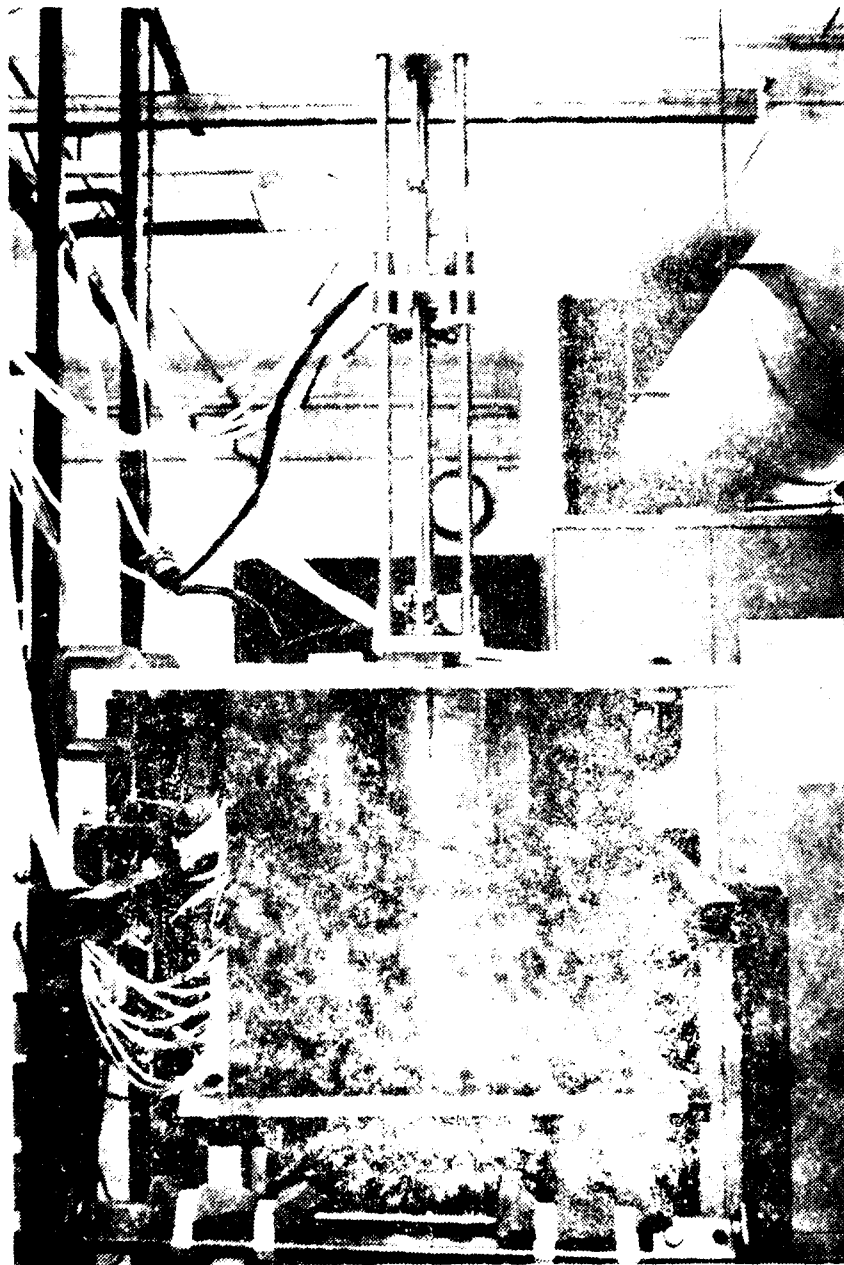


Figure 4. View of passage test rig looking into discharge of the passage, Task I.

bars riding in inner and outer slots in the endwall, could be positioned across the passage as desired and clamped to seal against flow leakage. The bars and slots necessarily extended beyond the sidewalls of the passage in order to keep the endwall sealed with the probe positioned toward either side. It was found that, although the slide bars fit tightly in the endwall slots and against the sidewalls, they could be easily positioned manually after having been lubricated with a light grease. No gasketing of the slide bars against the slots or as extra sealing against the upper edge of the sidewalls was found to be necessary. The lower endwall of the test section is made of 19-mm thick plexiglass plate for flow visualization and is attached to the lower edge of the sidewalls by quick-release bolts and mounting brackets for easy access to the flow passage. Dimensional details of the test section and traverse planes, and the coordinate scheme used for flow testing are given in Appendix A.

The sidewalls of the test section were made up of laminated mahogany boards. The sidewalls, which can be seen in the side view of the test section in Fig. 3, or in the view of the test section discharge in Fig. 4, are constant height of 40.6 cm and approximately 10 cm thick. Fabrication of the sidewalls posed a difficult machining problem because of the large work pieces involved and limited machine and milling cutter capacity. Machining was finally carried out by constructing each wall from three individually machined layer segments. In forming up the passage with the sidewall inner profiles a constant mean radius was maintained; however to help accelerate the flow through the bend, a slight contraction

in passage width, or cross sectional area, was incorporated through the full 90 degrees of the bend. The passage width, w , is given by the relation,

$$\frac{w}{w_0} = 1 - \frac{8}{\pi}(1-a)(4\alpha - \sin 4\alpha)$$

where $w_0 = w(\alpha = 0)$, and a is the (normalized) assigned width, $w(\alpha = \pi/2)/w_0$. With this relation, the transition in passage width between the bend and the constant width inlet and exit sections is continuous through the second derivative. In each of the 12 traverse planes, 16 static taps uniformly spaced in each sidewall along with the static tap fixture installed in the slide bar were used to obtain static pressure distributions. The back side of these taps can be seen in the side view of the test rig in Fig. 3. The static taps were constructed by cementing in place short segments of 16 ga. (1.2 mm I.D.) hypodermic tubing in drilled holes carefully aligned normal to the sidewall profile at the traverse stations. Care was taken that the inserted tubing was finished flush to the sidewall and the hole deburred to obtain a clean, sharp static tap.

As noted in the schematic of the test rig in Fig. 1, a transition section from circular to rectangular cross section followed by a boundary layer generator section and adaptor section introduce the flow into the test section. Again, these sections, which were constructed from molded fiberglass and plexiglass plate, can be seen in side view of the test rig in Fig. 3. The boundary layer generator section consists of a removable screen holder segment by which curved and/or slanted uniform mesh screens can be installed into the flow without disassembly of the test rig. Thus,

controlled, symmetric two-dimensional velocity profiles across the passage from one endwall to the other can be easily produced in the inlet flow to the test section. The following adaptor section has adjustable side-wall bleed doors to provide further control on the flow into the test section. Also in the adaptor section a pitot probe could be positioned to the center of the cross section of the passage to determine free-stream dynamic and static pressures, q_0 and p_{s0} , respectively. This was done when setting the flow rate; the pitot was of course removed prior to the actual testing. Generally, tests were run at a plenum gage pressure of approximately 235 mm H_2O , or corresponding maximum flow velocity into the test section for test results presented later of about 40 m/s. The test Reynolds number based on this velocity and the span of the passage cross section is 1.02×10^6 .

1.3. Data Acquisition and Experiment Control System

As a major effort of the present investigation, an automatic data acquisition and experiment control system was set up for tests using the large-scale, low-speed flow loop (see Ref. 1 for complete description of the data system). This system was designed with versatility and flexibility in mind for general application to testing programs in the laboratory. With this system, experimental data are recorded, stored, and instruments controlled automatically as programmed in the test procedure. In addition, data are collected at a high rate, facilitating on-line reduction of data and checking of experimental results; in the process, intervention of human error in data collection and reduction is, of course, minimized.

A schematic layout of the data system can be seen in Fig. 5. Unknown pressures supplied from the pressure probe, pressure reference system, or through the fluid switch as indicated are fed into the pressure scanner where a pressure transducer converts pressure differences into voltage differences. The voltage across the transducer is amplified, filtered and fed into the voltage scanner. By selecting the appropriate scanner channel, the amplifier output is connected as input to the digital voltmeter. Selection of other scanner channels provides the connection of probe position voltages to the voltmeter or the activation of the pressure scanner and probe positioner. Once the amplifier output is connected to the voltmeter, the voltmeter is triggered to take the measurement. The reading is then output to the system PET controller/computer.

Through appropriate programming of the PET, the pressure scanner is stepped to the next pressure line to repeat the measurement process. If probe positioning is instead required, the PET activates the positioner by closing specific channels on the voltage scanner. The collected data are processed and then recorded on either magnetic cassette tape or a disk storage system. Data may also be viewed on the CRT of the PET or printed out as hard copy.

The pressure reference system (Ref. 2) indicated in Fig. 5 provides high precision reference pressures for on-line calibration of the transducer in all test pressure measurements. Also, through the fluid switch indicated, different pressures may be supplied at various steps of the pressure scanner as reference for other pressure measurements. Necessary temperature measurements are also made using thermocouples.

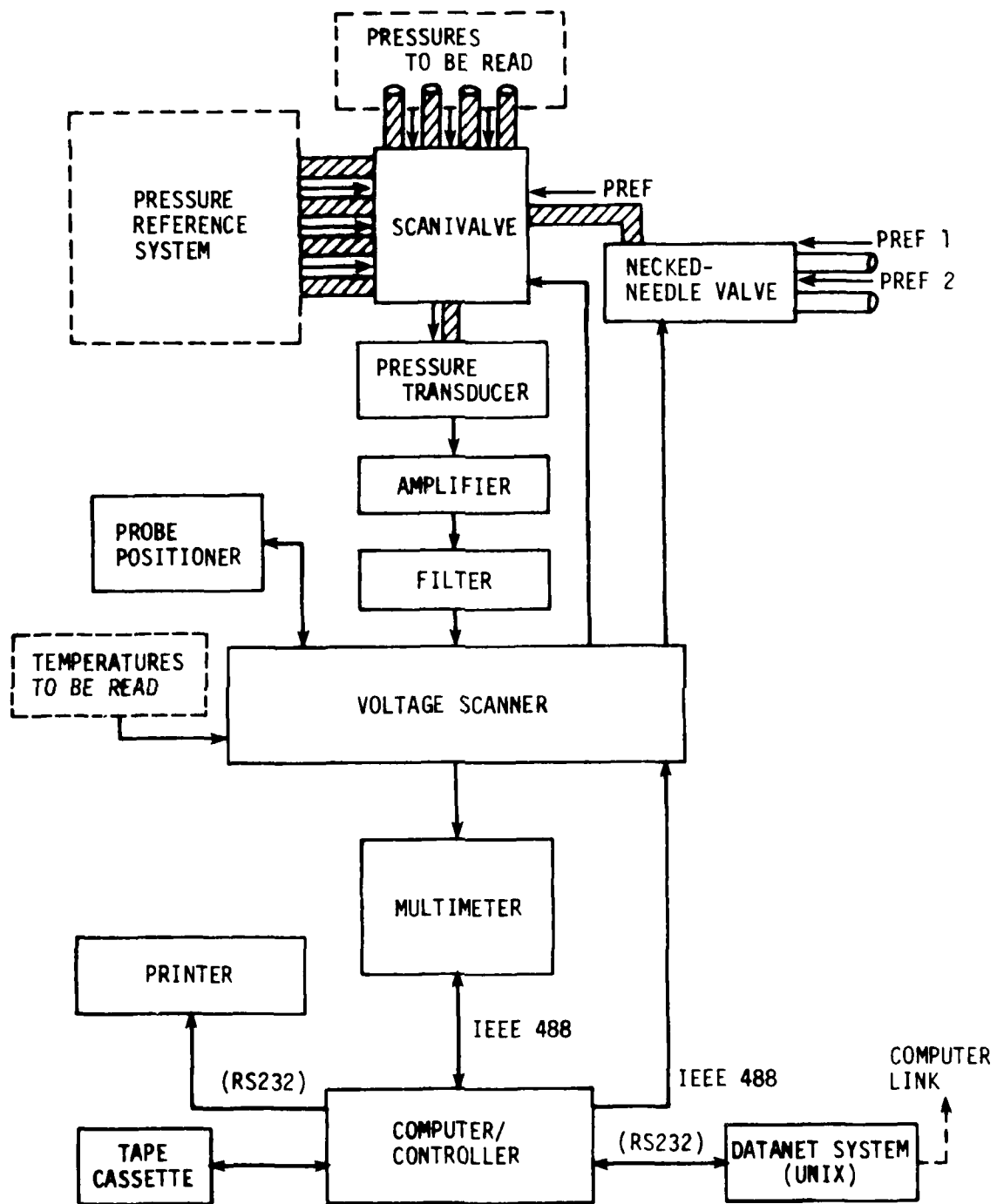


Figure 5. Functional diagram of data acquisition and experiment control system, Task I.

To illustrate the data system, a program designed to position a five-hole directional pressure probe in translation, to automatically null the probe in yaw, and to record probe pressure measurements along with associated pressure and temperature measurements is described in the flow diagram in Fig. 6. Raw pressure and temperature data only are collected by the program; further reductions of data to obtain total pressure, Mach number, flow pitch, etc., based on the five-hole probe calibrations (Ref. 3) are handled in other programs not described here. Pitot tube measurements in addition to the five-hole probe measurements are made in the program to obtain particular reference values for the flow as needed in data reduction.

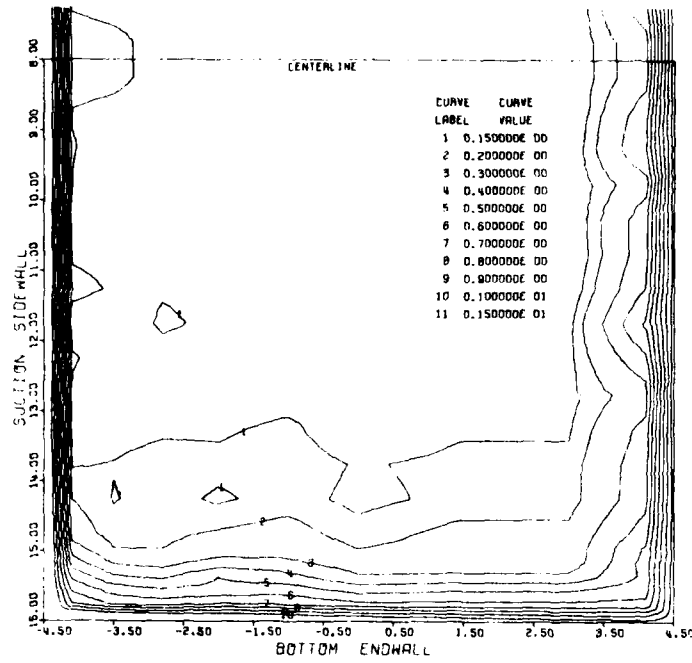
The program is made up of five major parts as implied in the flow diagram by the five branches from the main program. These parts are: (1) calculation of five-hole probe positions for translations, (2) pitot tube measurements, (3) probe translation, (4) automatic yaw-nulling of probe, and (5) collection of probe pressure and temperature measurements. Operation of the program is essentially left-to-right across the flow diagram, with positioning of the probe and measurement of pressures (shown toward the right-hand portion of the diagram) carried out sequentially over all the previously calculated probe positions. On-line calibration of the pressure transducer for pressure vs. voltage carried out for each spin of the pressure scanner provides high accuracy in all pressure measurements.

The data system involving the PET computer as just outlined, is a self-supporting system entirely controllable through appropriate programming. In addition, through use of an RS232 serial adaptor (see

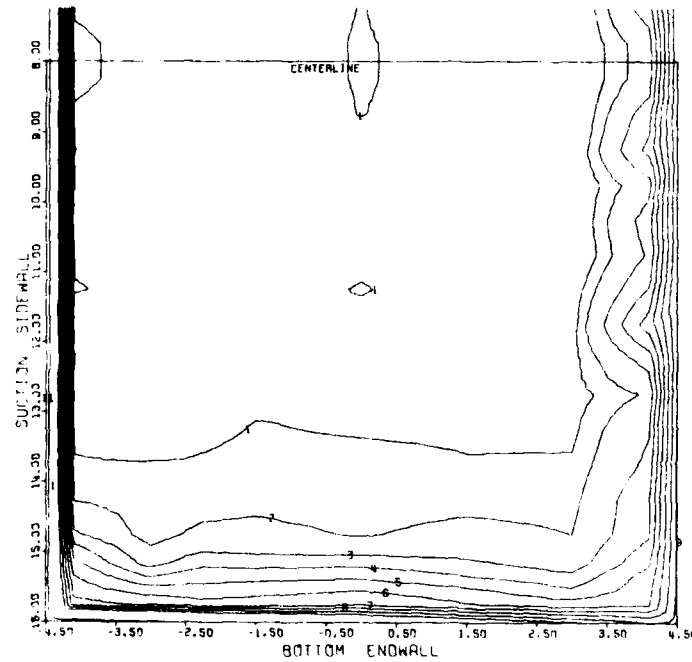
again Fig. 5) the PET can be operated as a remote terminal in the University Computational Center DATANET system. This latter system, incorporating a PDP 11/34 computer and high-capacity disk units, is a university-wide high-speed recirculating digital network of mini- and microcomputers in experiment control and data acquisition. A file management system called (UNIX) (see Ref. 4), is used for collection of experimental data and program files, and assembled object code can be directly down-loaded into the remote terminals for subsequent execution. Furthermore, a data link exists between DATANET and the University mainframe computer which provides an even further expanded data reduction and computing capability.

1.4. Presentation and Discussion of Experimental Results

Experimental results obtained with the test passage are presented in Figs. 7 through 10. These plots, based on preliminary results of testing carried out to date, are for selected traverse planes through the passage. Contour plots of total pressure coefficient, static pressure coefficient, and Mach number are shown along with vector plots of in-plane (traverse plane) velocities. In traversing the five-hole pressure probe, 21 points were measured from endwall to endwall to record yaw and pitch angles of the flow and impact pressure. This procedure was carried out for 8 or 9 slide bar positions in each plane, with these positions concentrated mainly toward the suction sidewall. Static (or total) pressures obtained with the sidewall and endwall taps were combined with the traverse data to complete the experimental results per traverse plane. A summary of the data collection, reduction formulas, coefficient definitions and coordinate system used is contained in Appendix A. In

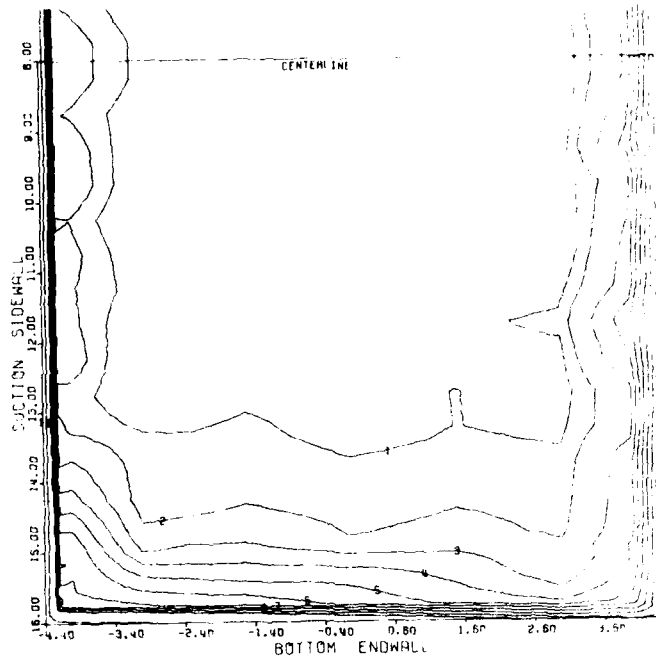


(a) Plane 1 (Inlet)

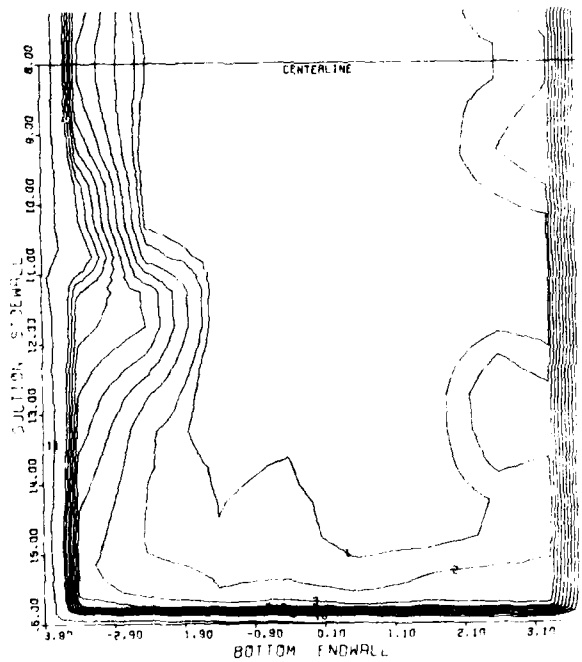


(b) Plane 2 (15 deg)

Figure 7. Experimental contours of total pressure coefficient C_{pt} for selected traverse planes in passage test rig, Task I. $[C_{pt} = (p_{to} - p_t)/q_0]$

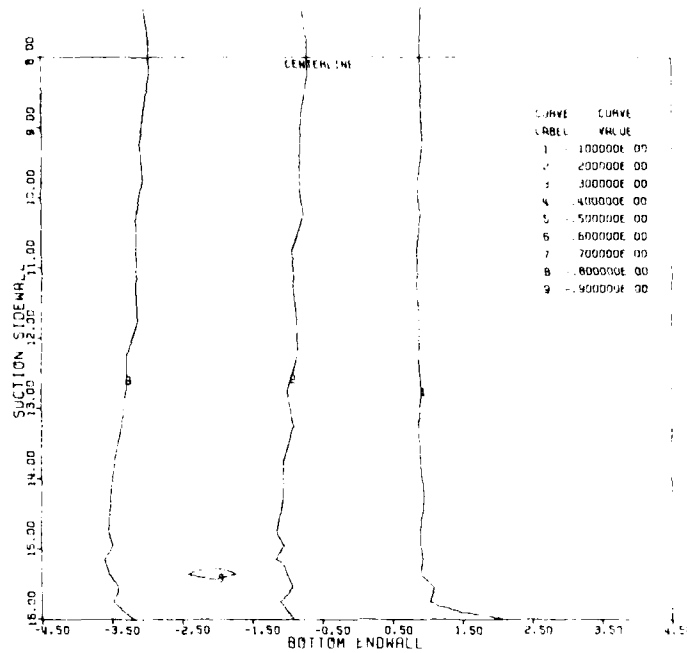


(c) Plane 6 (75 deg)

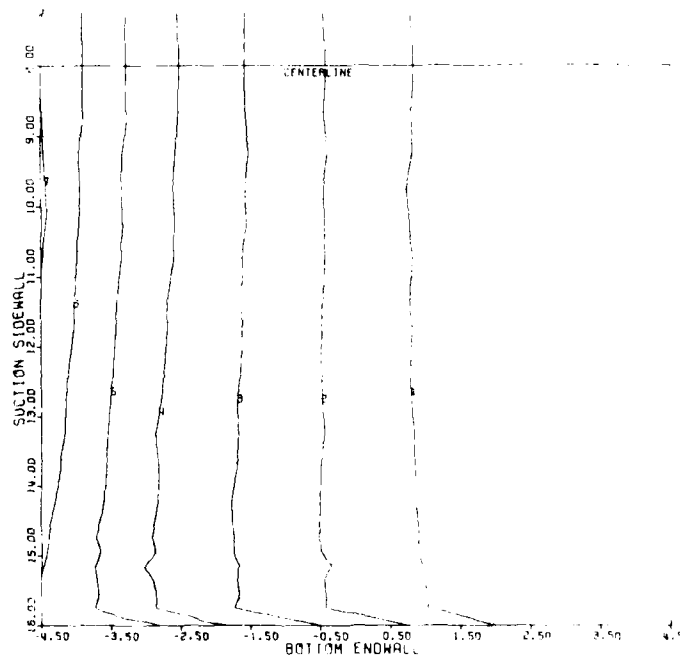


(d) Plane 7 (90 deg)

Figure 7. Concluded.

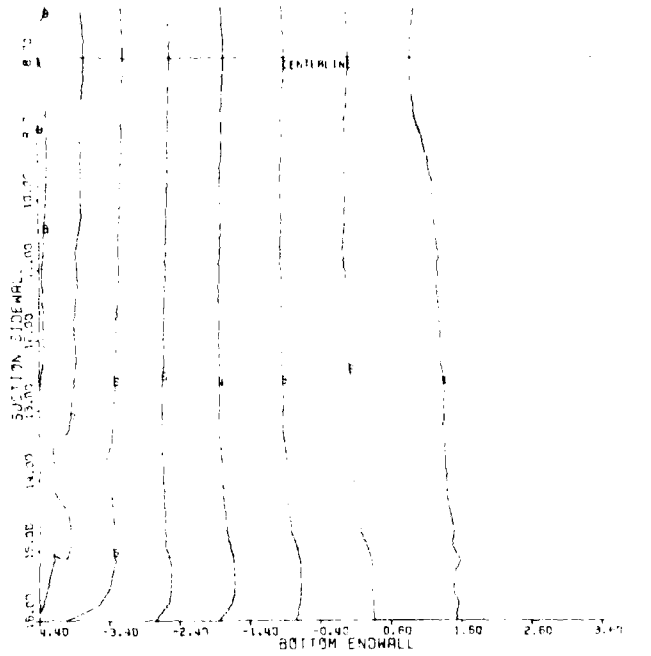


(a) Plane 1 (Inlet)

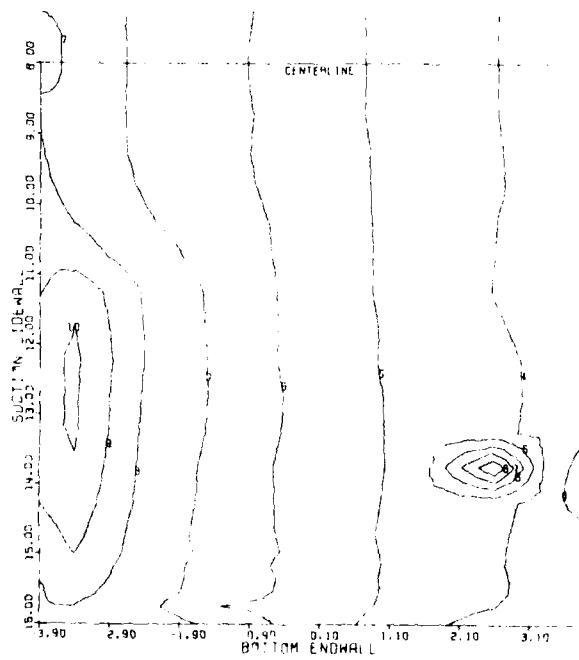


(b) Plane 2 (15 deg)

Figure 8. Experimental contours of static pressure coefficient C_{ps} for selected traverse planes in passage test rig, Task I. $[C_{ps} = (p_s - p_{so})/q_o]$

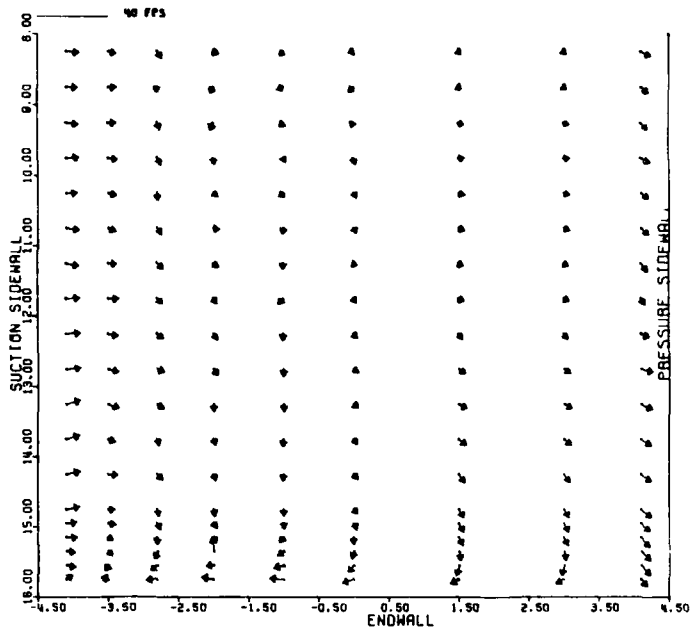


(c)Plane 6 (75 deg)

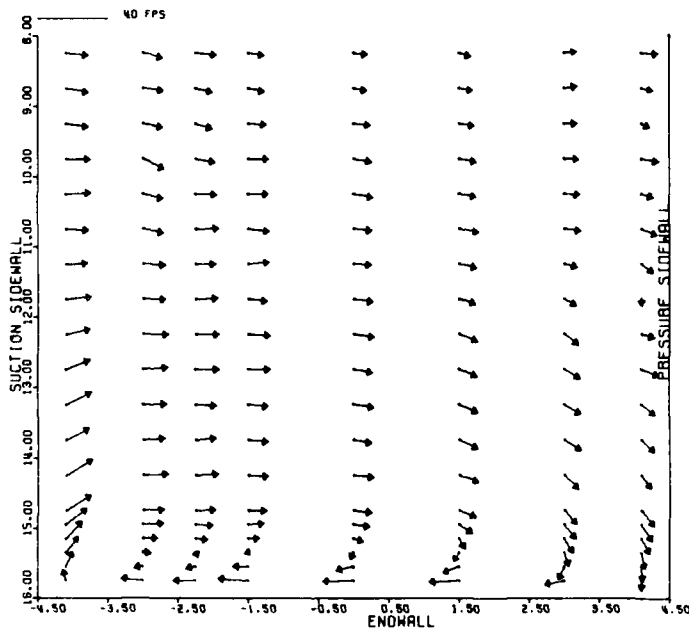


(d)Plane 7 (90 deg)

Figure 8. Concluded.

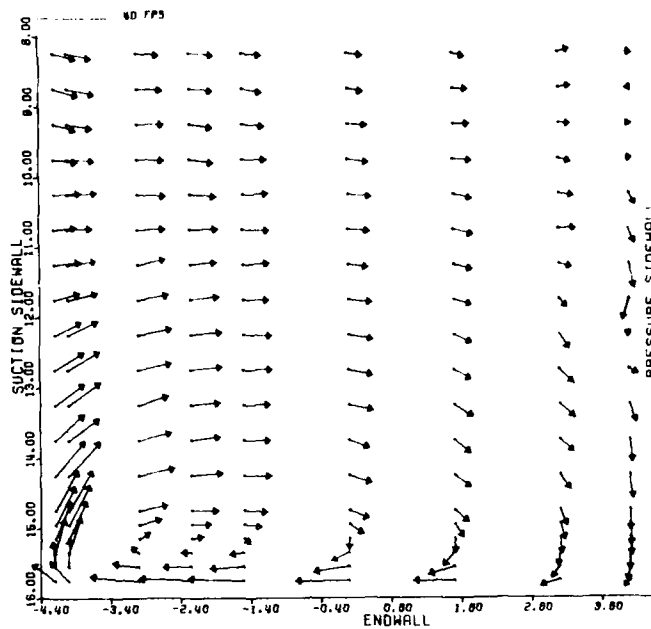


(a) Plane 1 (Inlet)

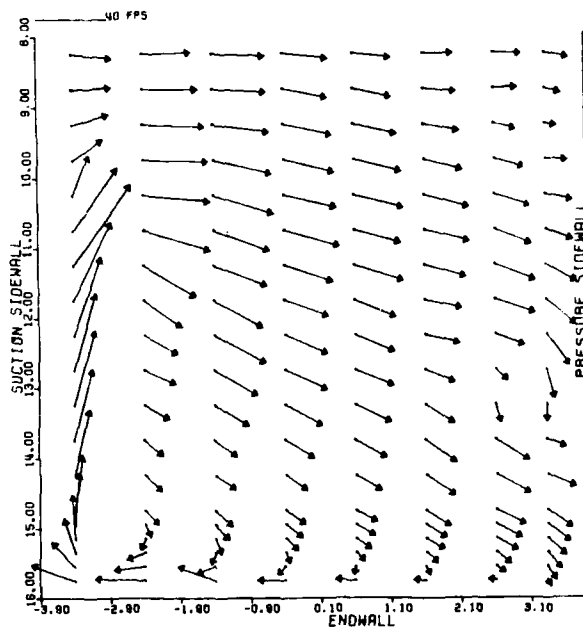


(b) Plane 2 (15 deg)

Figure 9. Experimental in-plane flow velocity vectors for selected traverse planes in passage test rig, Task I.

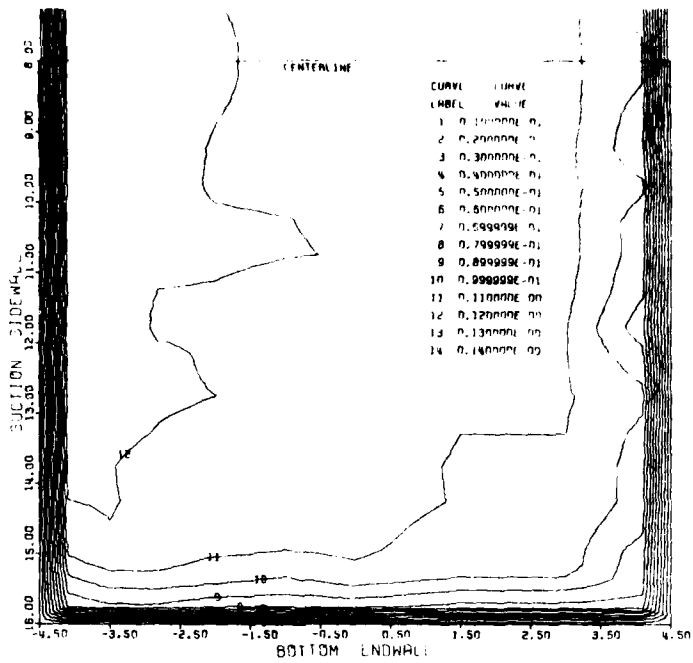


(c) Plane 6 (75 deg)

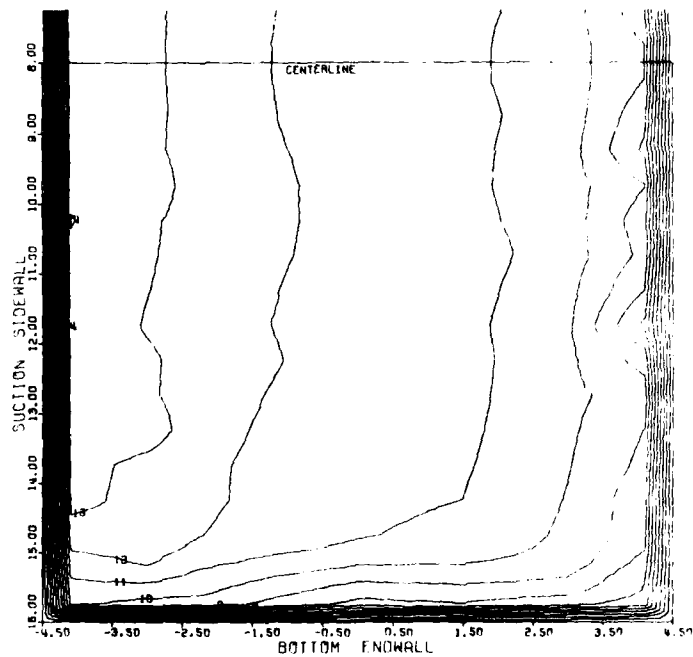


(d) Plane 7 (90 deg)

Figure 9. Concluded.

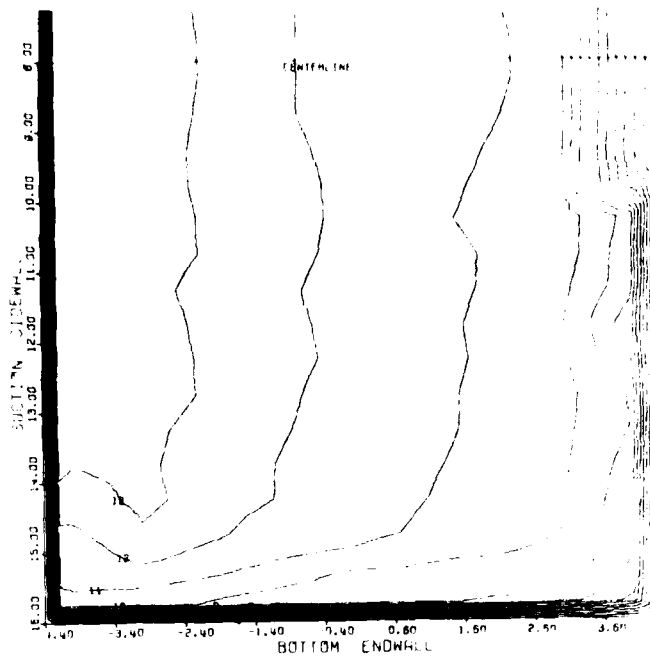


(a) Plane 1 (Inlet)

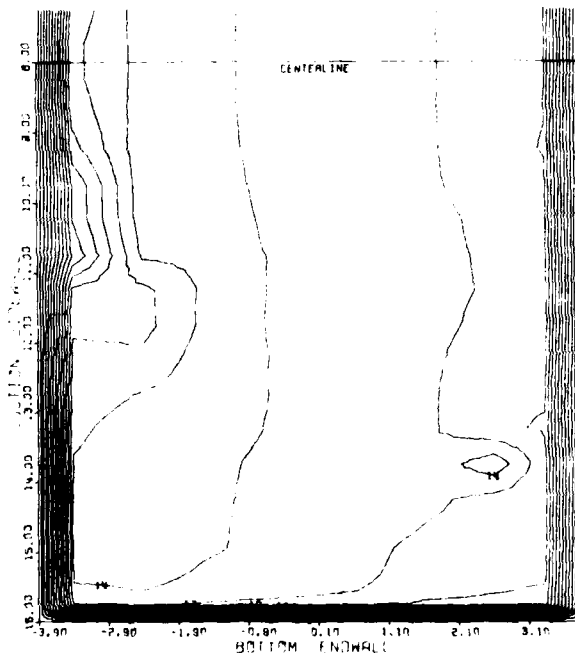


(b) Plane 2 (15 deg)

Figure 10. Experimental contours of Mach number for selected traverse planes in passage test rig, Task I.



(c) Plane 6 (75 deg)



(d) Plane 7 (90 deg)

Figure 10. Concluded.

generating the contour plots shown, enrichment of the measured data was employed by interpolating at two intermediate points in both the x and z coordinate directions, and also by carrying out extrapolation into the corners of the traverse planes.

Since the velocity profile generated from endwall to endwall entering the test passage was symmetric about the center plane of the passage, results are shown only for the lower half of each traverse plane. The entering sidewall boundary layers were thin, while the entering endwall boundary layers were relatively thick, producing strong vortical motions in the main stream direction throughout the passage. The movement of low energy fluid as the flow proceeds through the bend and discharge sections can be traced readily in terms of successive plots such shown in Figs. 7 through 10. Also flow visualizations were made by producing ink traces on the lower endwall and both sidewalls to help in analyzing the flow and to guide in interpreting measured probe data. Such flow visualization produces the patterns of limiting streamlines on the passage walls and in many cases may or not indicate flow directions interior to the passage close to the walls because of possible skewing in the boundary layers in regions of high shear. These patterns showed, as expected, very strong cross-flow on the endwalls from pressure side to suction side with consequent interaction with the flow on the suction sidewall along a separation line. However, no evidence was seen of three-dimensional separation of the entering boundary layer itself from the endwall which has been found to predominate the flow through cascades (See Refs. 5, 6).

The plots shown in Figs. 7 through 10 are of the flow in selected traverse planes viewed from downstream, with the suction sidewall on the left and the pressure sidewall on the right. The traverse planes represented are the inlet, 15-deg, 30-deg and 90-deg planes through the bend. In Fig. 7 the development of total pressure loss coefficient, C_{pt} , can be seen. The higher values of total pressure loss corresponds to higher values of C_{pt} or contour label. In the inlet plane (plane 1) the Bernoulli surfaces in the entering collateral endwall boundary layer are evident, with some effect of the bend already being felt in growing of the pressure side boundary layer. Nothing is concluded about the flow on the suction sidewall at this point, since the limiting position of slide bar 1 prevented traversing the five-hole probe close enough to the suction side. The contours of C_{pt} in traverse planes 2 and 3 are very similar to those in plane 1, showing little development of losses through the first 30 degrees of the bend. By plane 7, at 90 degrees in bend, we can see an increase in loss level along with thinning of the endwall layer in combination with the strong interaction of the endwall and sidewall flows high on the suction side. Also in plane 7, the pressure sidewall layer has by this time apparently again decreased in thickness.

Figure 8 shows contour plots of static pressure coefficient, in which local static pressure, p_s , is referenced to the pitot static and dynamic pressures p_{s0} and q_0 , respectively, for the entering velocity profile. These contours, running vertically from endwall to endwall, correspond to those for potential flow over the great majority of the passage for planes 1 through 3, but with increasing pressure gradient across the passage from suction side to pressure side. The center of low pressure,

in plane 7, has moved off the section sidewall out into the flow along with formation of the passage vortex near the suction side. The overall gradient of pressure from sidewall to sidewall has now decreased in response to the action of the losses in the flow. Also, an extraneous vortex filament is evident from the local low pressure center near the pressure sidewall. Further testing of the flow is needed to explain this.

In Fig. 9 we see the in-plane velocity component in the four traverse planes. For the inlet plane, although these components are small, on the order of 0 to 5 or 6 ft/s, there is indication of downward flow on the pressure side and across the endwall toward the suction side, with possible starting of the passage vortex in the suction side corner at the endwall. In planes 2 and 3 the probe traverse closest to the suction sidewall is still outside the boundary there as indicated by the in-plane velocity vectors pointing essentially outward from the wall. Also in plane 3 there is a slight indication of flow across the centerline from the upper half of the passage. For planes 2, 3 and 7 the strong secondary flow formation in development of the passage vortex is seen.

In Fig. 10 of Mach number contours, planes 1, 2, and 3 show limited secondary flow action, except for the spanwise velocity gradients caused by the passage curvature. In plane 7, however, the low energy region in the suction-side corner is being wrapped up into the passage vortex that forces itself down into the corner. Again we see evidence of the extraneous vortex near the pressure-side corner. Plane 7 also shows an overall increase in average velocity which is caused by the convergence of the passage cross section.

2. TASK II: EVALUATION AND MANAGEMENT OF UNSTEADY FLOW EFFECTS IN
AXIAL-FLOW COMPRESSORS

In order to further our knowledge and experience involving unsteady flow effects in axial-flow compressors acquired under AFOSR grant 76-2916 a detailed review of related literature was started in the Fall of 1978 and continues. Also, more experiments were completed on the three-stage research compressor used previously (see Figure 11). The conclusions reached by the beginning of 1979 are documented in Reference 7. Subsequent progress in Task II achieved under AFOSR Contract F49620-79-C-0002 is summarized in the following paragraphs.

A note about the data that will be described below may be helpful. Time-average results were acquired with slow responding instruments and represent the average value, over time, of a continuously measured quantity. Periodic-average results involve the average value of a periodically (e.g. once per rev) sampled quantity. Blade-to-blade-average results are the spatially integrated values of blade-to-blade profiles of either time-average or periodic-average quantities. Time-average results are independent of rotor sampling position while periodic-average results are generally not.

To ascertain whether or not varying the relative circumferential positions of the blades (same number in each row) of the inlet guide vane (IGV) and stator rows of the three-stage research compressor would result in measurable time-average stator performance (deviation angle and total-head loss) changes, the compressor was operated at 2400 rpm and local time-average total-head measurements were acquired for two different circumferential position settings of the IGV and first stator rows. At a lower rotor speed (1400 rpm), similar tests indicated an appreciable difference in inlet noise

PROBE
MEASUREMENT
STATIONS

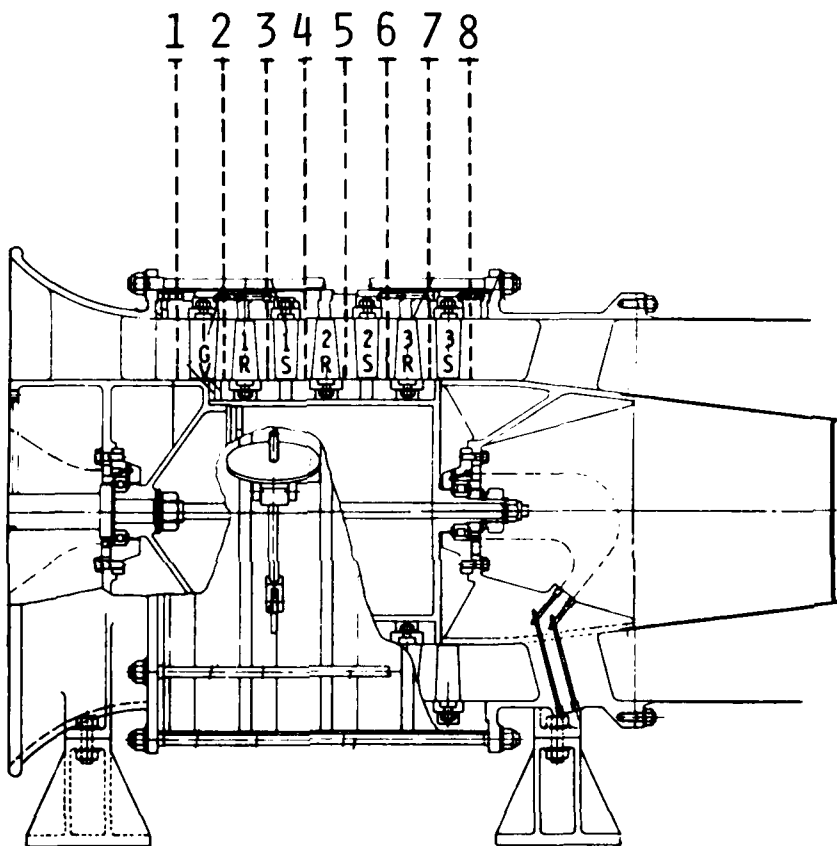
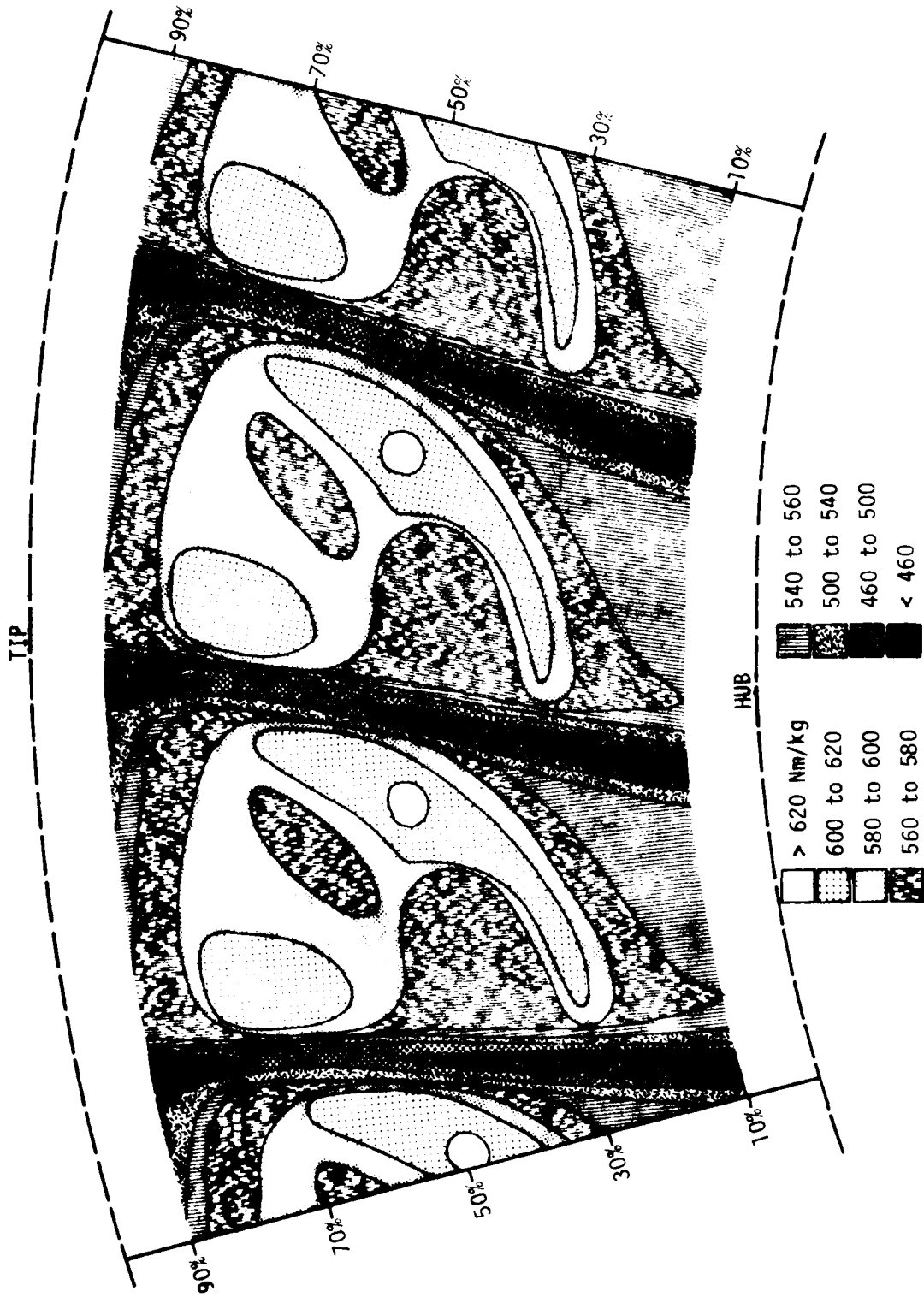


Figure 11. Research compressor with probe measurement stations.

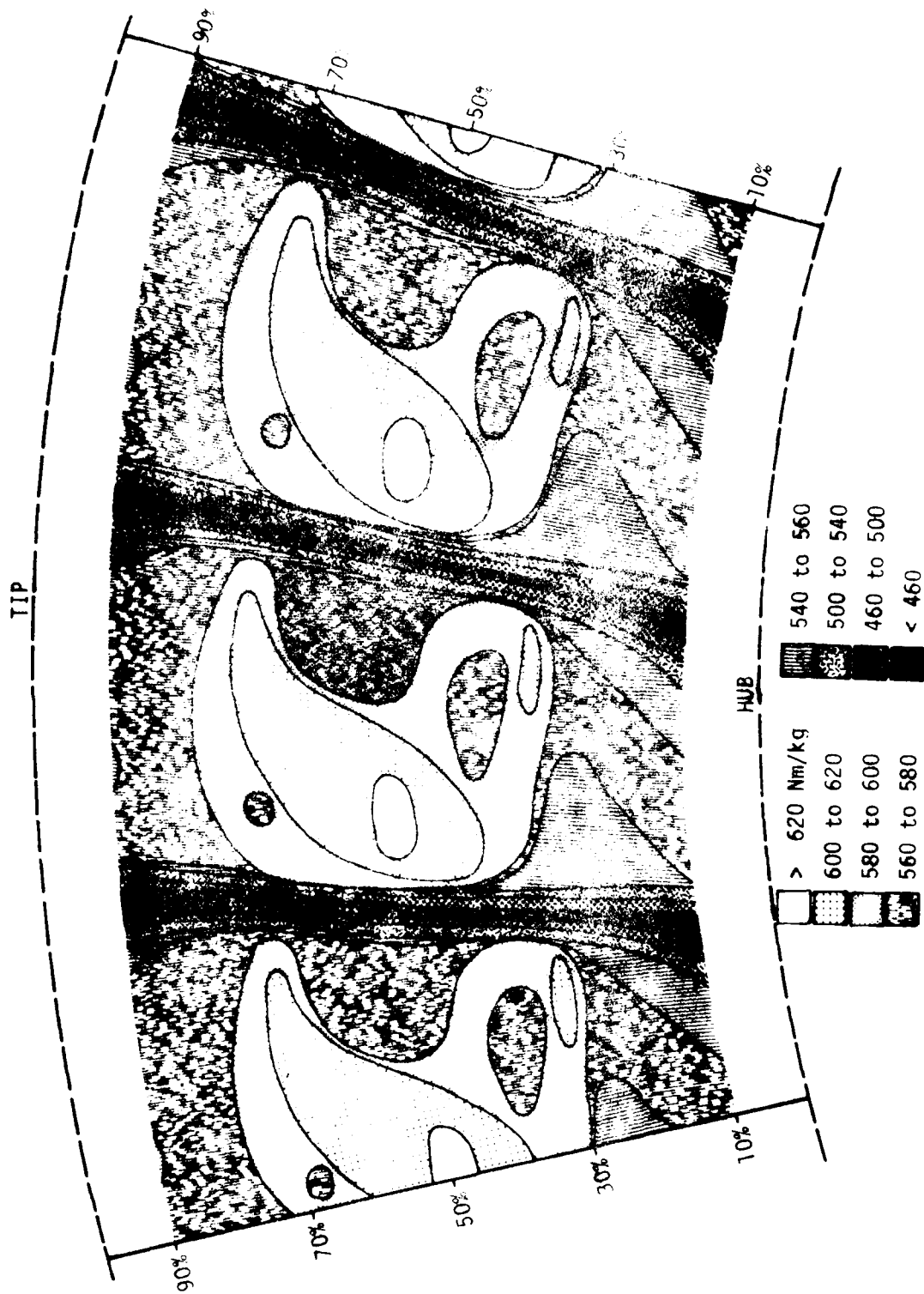
(about 6dB in the octave bands nearest the blade passing frequency) for different relative circumferential positions of the IGV and stator rows. However, time-average total-head loss and deviation angle data were inconclusive about stator performance differences. At the higher rotor speed, minimum and maximum noise circumferential positions of the IGV and first stator rows involved a difference in noise-sound pressure level of about 10 dB in the octave band including the blade passing frequency. Contour graphs of the time-average total-head measurements behind the first stator are displayed in Figure 12. Blade-to-blade-average values of the information in Figure 12 at various radii are compared in Figure 13. Representative time-average yaw angle data are shown in Figure 14. The blade and measurement position parameters are explained in Figure 15. Although the annulus cross-section distribution of stator exit local time-average total head varies appreciably with change of relative circumferential positioning of IGV and stator blades the blade-to-blade-average total-head values do not. Also, the stator exit free-stream angles do not seem to depend significantly on circumferential positioning of the IGV and stator blades. Thus it appears as if the circumferential placement of IGV and first stator blade rows relative to each other did not result in measurable stator performance differences under the present test conditions.

A fast-response total-pressure probe was used with a periodically sampling and averaging measurement system to observe the details of unsteady total-pressure variations in the first stage discussed above. The compressor was operated at the minimum-noise, 1400 rpm condition used in earlier studies. Details of the research are documented in Reference 8. In general, periodic-average total-pressures varied appreciably with rotor sampling



(a) MINIMUM NOISE CIRCUMFERENTIAL POSITIONING, $Y_{0IGV/S_S} = 0$, $Y_{0IS/S_S} = 0.159$

Figure 12. Local time-average first stator exit flow total-head variation with stator/IGV circumferential positioning (2400 rpm).



(b) MAXIMUM NOISE CIRCUMFERENTIAL POSITIONING, $Y_{01GV/S_S} = 0$, $Y_{01S/S_S} = 0.719$

Figure 12. Concluded.

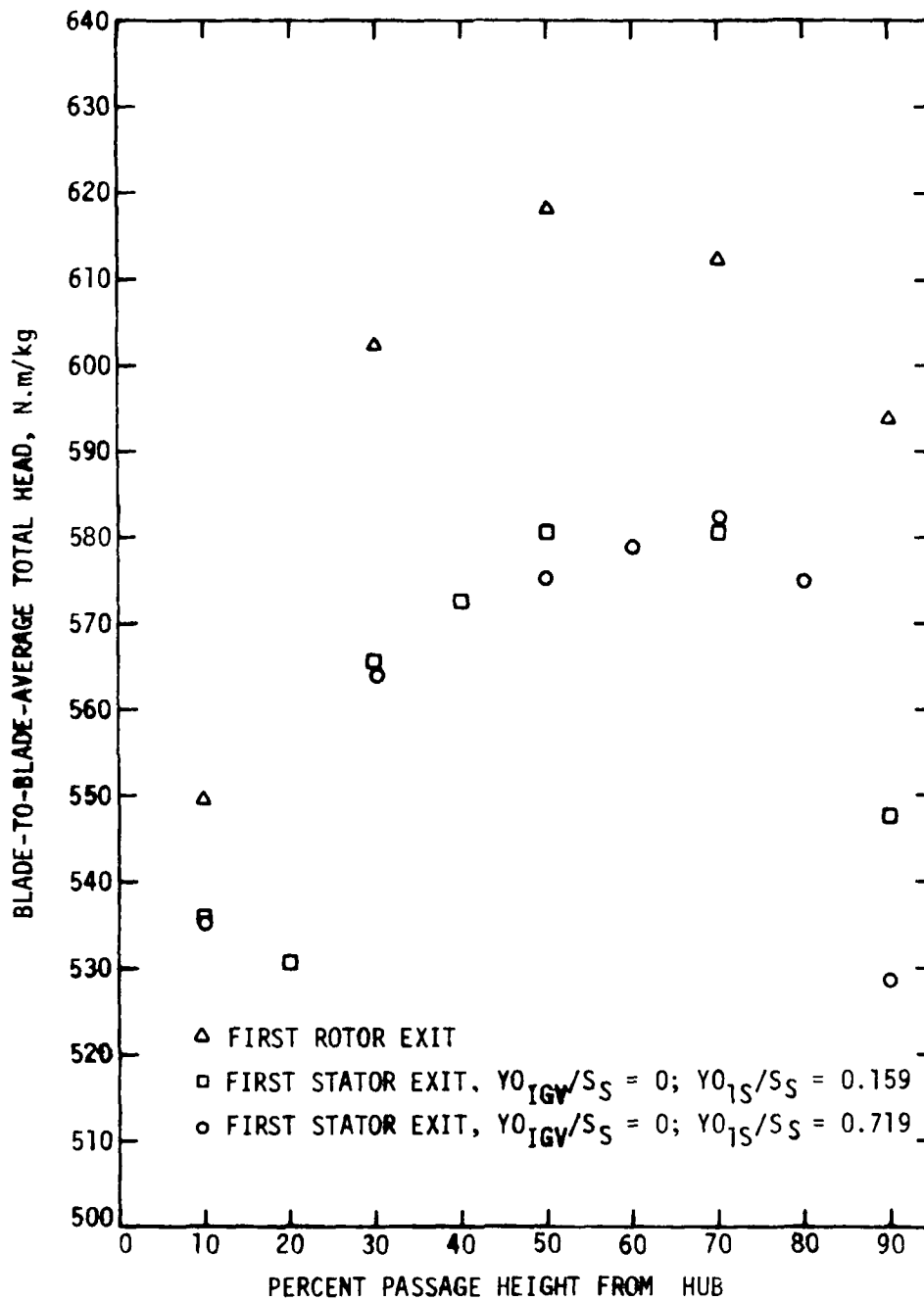
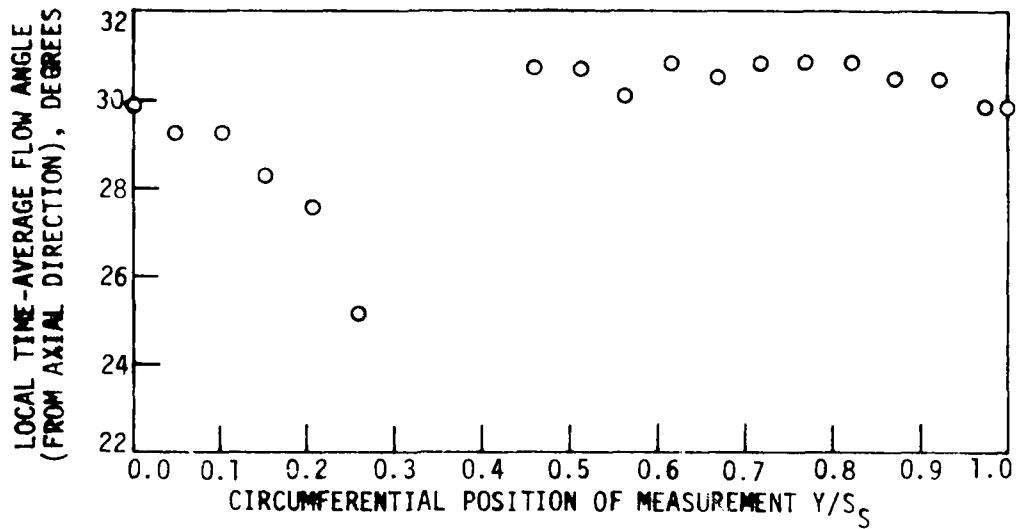
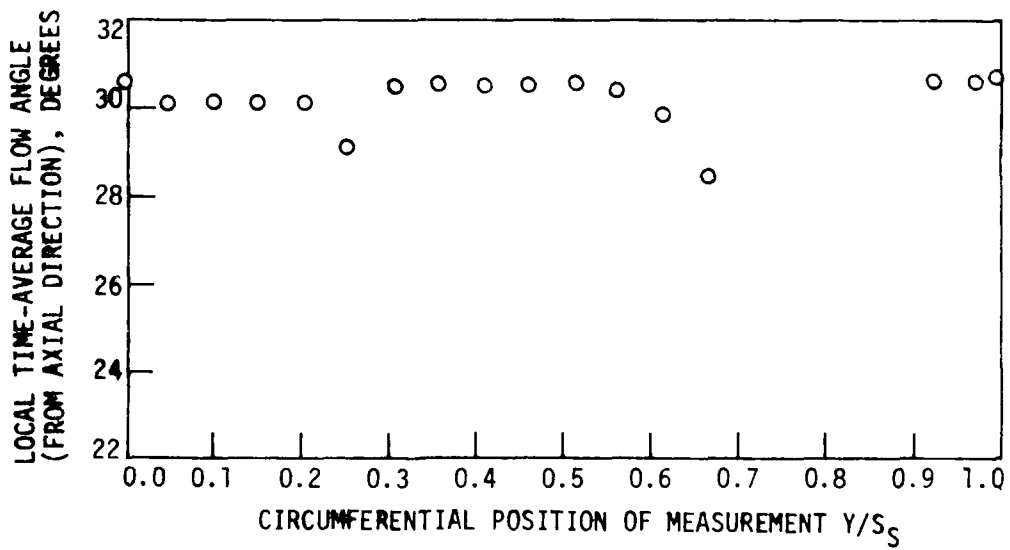


Figure 13. Blade-to-blade-average first stator exit flow total-head variation with stator/IGV circumferential positioning (2400 rpm).



(a) $YO_{IGV}/S_S = 0$; $YO_{1S}/S_S = 0.159$



(b) $YO_{IGV}/S_S = 0$; $YO_{1S}/S_S = 0.719$

Figure 14. Time-average first stator exit flow angle variation with stator/IGV circumferential positioning at 50 percent passage height from the hub (2400 rpm).

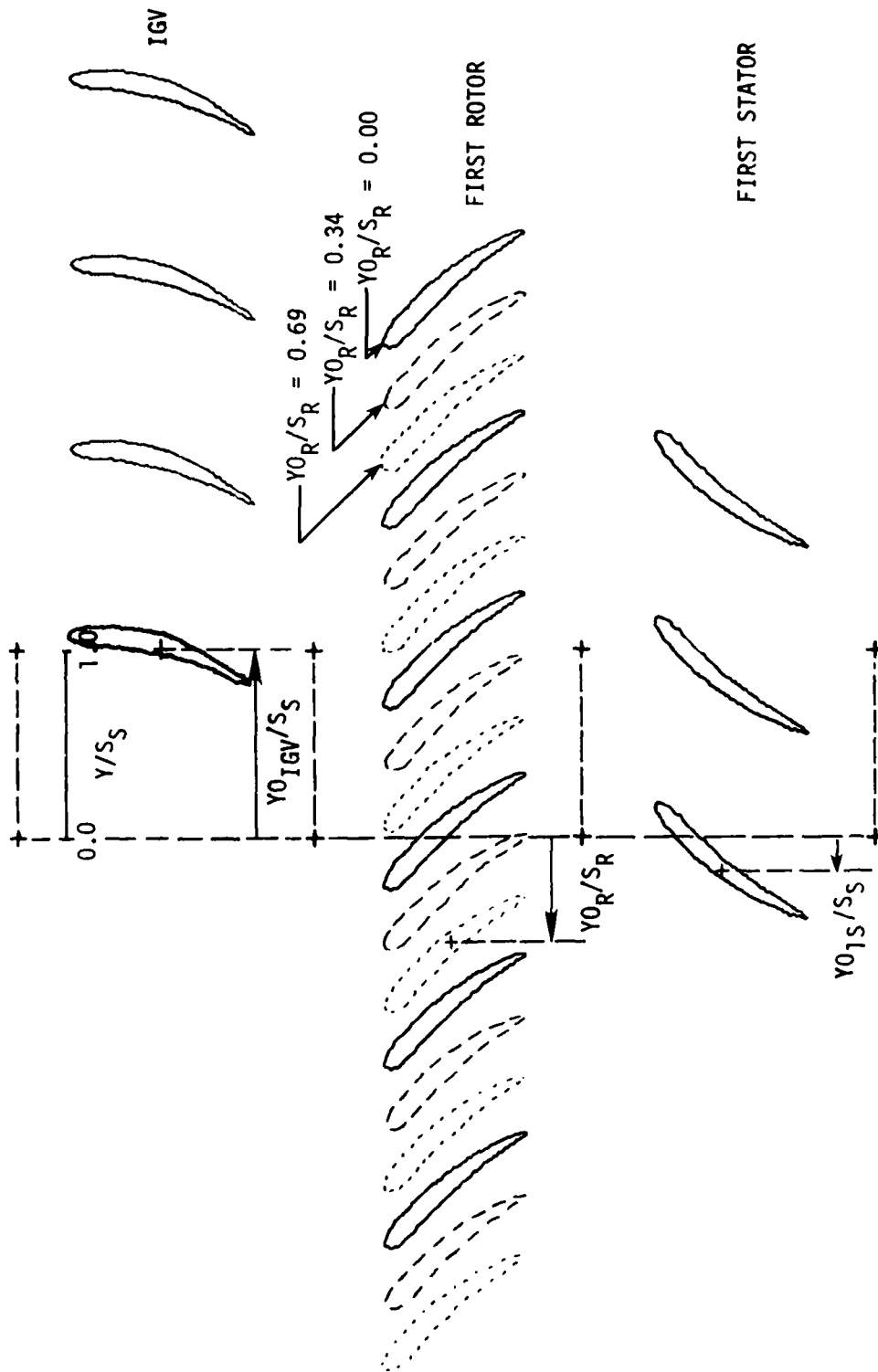
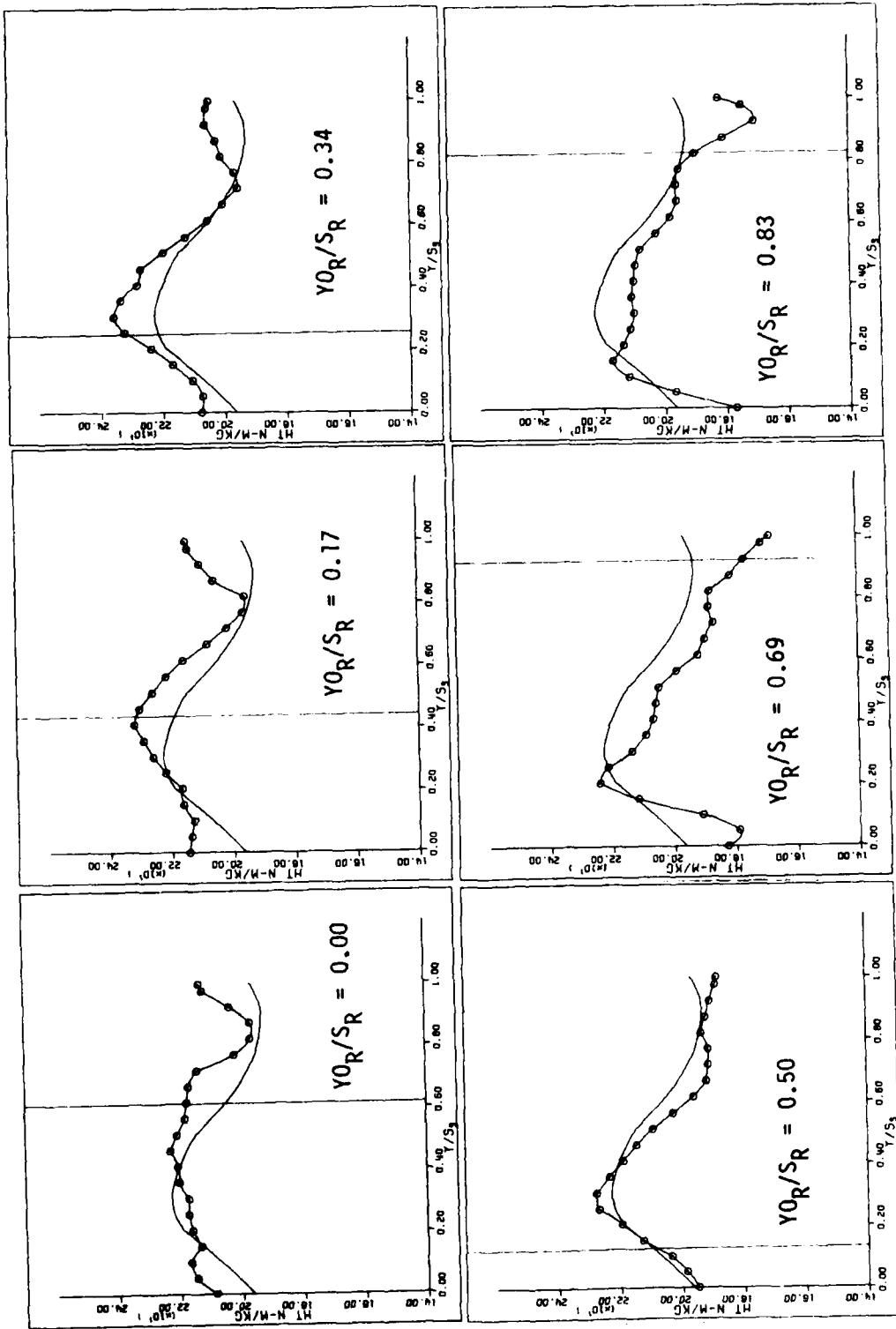


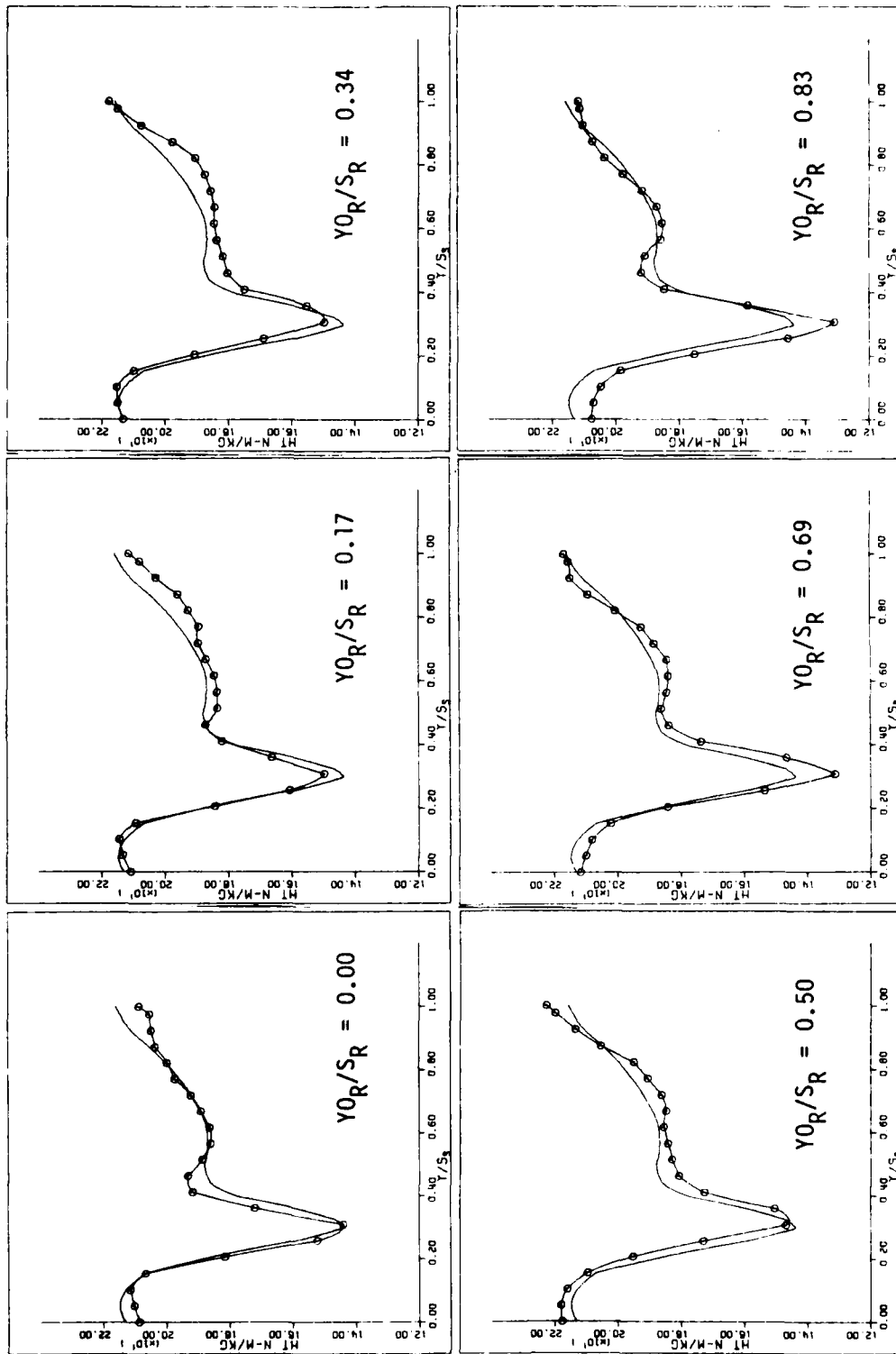
Figure 15. Blade cascade showing relative positions of blades for several rotor sampling positions. (S_R is rotor blade spacing; S_S is stator blade spacing; Y is measurement circumferential location; $Y0_R$ is reference rotor blade circumferential location; $Y0_{1S}$ is reference first stator blade circumferential location.)

position downstream of the first and second rotors but very little downstream of the first stator. Some of the data acquired at mid-span that demonstrate this observation are shown in Figures 16 and 17. Figures 16(a), (b) and (c) involve comparisons of local periodic-average and time-average total pressures. Figure 17 involves a comparison of blade-to-blade averages of the periodic-average and time-average total-head profiles shown in Figure 16.

Similar behavior was noted at other span locations. The trends in total-pressure unsteadiness could be explained in terms of the blade-wake chopping, transport and interaction kinematics model proposed in Reference 9. Since total-pressure values are indicative of fluid particle energy addition through work and energy loss through friction, Table 1 could be organized as shown to help explain what was observed downstream of rotors 1 and 2. The periodic-average total-head profile shape and magnitude downstream of the rotors seemed to reflect the different kinds of particles of fluid identified in Table A that were in the measurement window (between the +'s in Figure 15) for any rotor sampling position. Periodically varying spatial distributions and proportions of the different kinds of fluid particles at the measurement window resulted in differing total-head profiles. This kind of periodic fluctuation was not as prominent behind the stator, largely because all fluid particles lost energy only in the stator row.

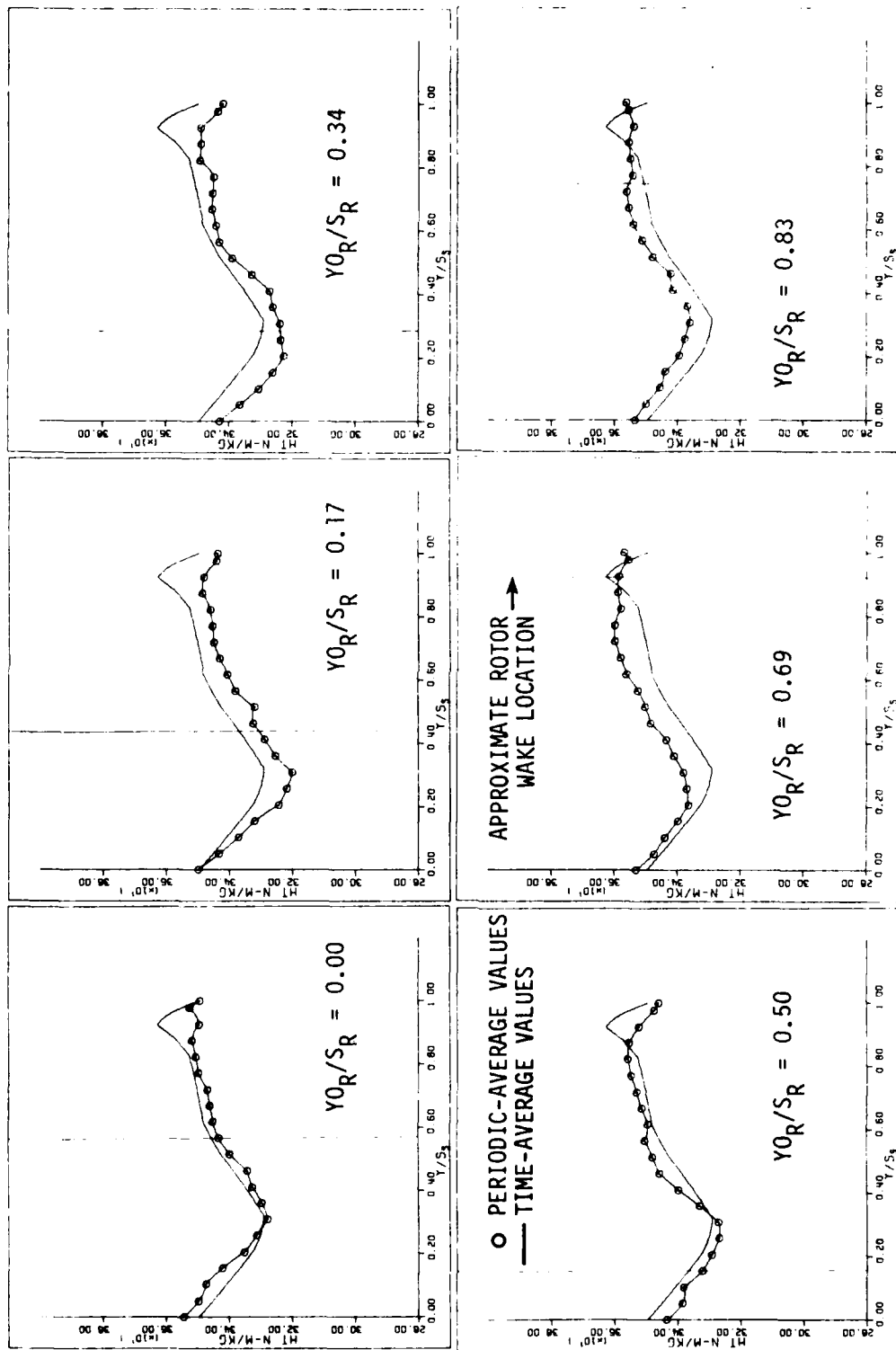


(a) first rotor exit, midspan
 Figure 16. Blade-to-blade distribution of periodic-average total head and time-average total head.



(b) first stator exit, midspan

Figure 16. Continued.



(c) second rotor exit, midspan

Figure 16. Concluded.

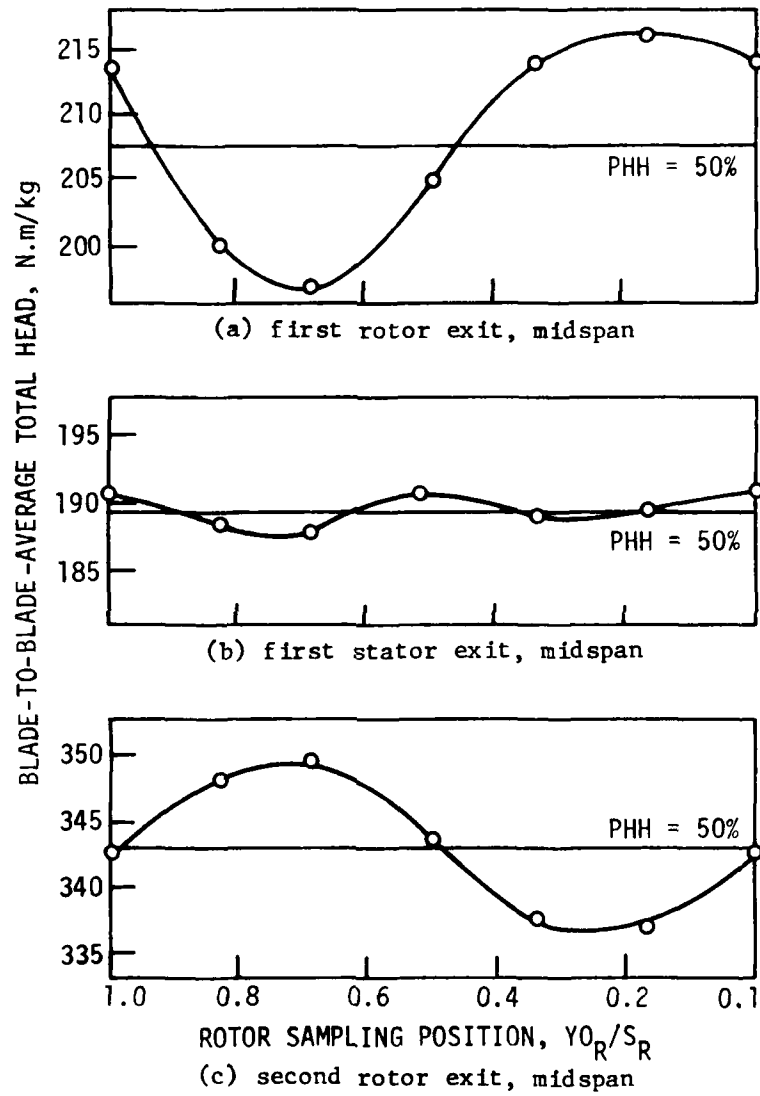


Figure. 17. Blade-to-blade-average total-head data.

Table 1. Behavior of fluid particles moving from the rotor inlet to the measurement station downstream of the rotor

Type of fluid particle	Total pressure at the rotor inlet	Energy added	Losses	Total pressure at the rotor exit measurement station
Freestream	A	B	C	D
Chopped IGV wake	<A	>B	>C	>D
Noninteracted rotor wake	A	>>B	>C(50%-90% PHH)	>D
			>>C(30%)	D
			>>>C(10%)	<D
Interacted rotor wake	<A	>>B	>>>C	<<D

The freestream values are set arbitrarily at levels A, B, C and D. Other values are estimated in terms of being less than, equal to, or greater than these reference values.

3. TASK III: DEVELOPMENT OF A DESIGN-SYSTEM ORIENTED DEVIATION ANGLE PREDICTION EQUATION FOR ADVANCED COMPRESSOR AND FAN CONFIGURATIONS

Earlier analytical (USAF/AFAPL Contract F33615-76-C-2090) [Ref. 10] and computational (NASA Grant Nsg-3033) [Ref. 11] work suggested a correlation of compressor and fan cascade-flow turning angles with blade-profile boundary layer development characteristics. The results of these investigations were integrated and extended (USAF/AFOSR Grant 78-3609) to cover more challenging test cases including more of the variables existing in real compressor flows. Task III of the current contract was directed toward the development of a design-system quality deviation angle prediction equation for advanced compressor and fan cascade configurations.

It was found in Reference 10 that there were few cascade data sets available with adequate information to give insight into the nature of the interaction of the boundary layer characteristics and the blade cascade deviation angle. Therefore, the computation method of References 11 and 12 was used in the current investigation to predict the blade-to-blade passage boundary layer development characteristics and the outlet fluid flow angles for typical cascade geometries. Test configurations which involved many of the variables existing in real compressor flows were chosen. Each test case included some experimental data which was used to verify the validity of the computational model.

Several changes were made in the original computer program to better model the additional test configurations. A new differentiation scheme was used to determine the surface pressures near the trailing edge of the blade. This differentiation method provided smoother and more consistent surface pressure distributions than did the previous spline fitting method. The better estimation of surface pressures also improved calculation convergence.

The program was also modified to model small regions of supersonic flow. The modification, suggested and outlined by Jerry Wood of the NASA-Lewis Research Center, has proven to be useful, though when compared to experimental data it underestimates the peak Mach number. The total-pressure loss model of Reference 11 and 12 was also modified to account for changes in the thickness and the radial location of the streamsheet downstream of the trailing edge.

A total of eight test cascade configurations involving a wide range of variables were selected. The variables included incidence angle, inlet Mach number, inlet Reynolds number, and axial-velocity density ratio (AVDR). Table 2 shows the test configurations and the significant variables for which computations were made.

The double circular arc cascade [Ref. 13] provided insight into the effect of the axial velocity-density product ratio (AVDR) on the flow field. Figures 18 and 19 show the large discrepancy which can exist between the surface pressures if the distribution of AVDR is not correctly modeled. Additional insight into the effect and distribution of AVDR was gained through discussions with H. Starcken of the DFVLR. The importance of determining whether the AVDR reported in experiments corresponds to a ratio taken between exit and inlet measuring stations or between trailing and leading edge averages was verified by computation. This ratio has a particularly significant effect on pressure distribution, turning and loss for high-diffusion-ratio cascades.

Variation of incidence for the 10A30/27.6 π 45 cascade [Ref. 14] produced computed fluid turning which was similar to that experimentally measured. The experimental measurements also included the distribution of

Table 2. Test configurations and significant variables tested.

Blade Section	Reference	Angle (deg)	T	P ₁	P ₂	Experimental Data Available		Significant Variables Tested
						Flow Field Measurements	Boundary Layer Characteristics	
Double Circular Arc: $\theta = 90^\circ$	13	15	1.629	0.6	1.267 $\cdot 10^6$	•	•	Incidence Mach number
10A10/27.0745	14	27.4	1.3	0.4-0.85	3.7-7.0 $\cdot 10^5$	•	•	Incidence Mach number
65-(12)10	15	45.7	1.0	0.13-0.06 0.8-0.9	3.2-1.3 $\cdot 10^5$ 1.3-2.3 $\cdot 10^6$	•	•	Reynolds number Mach number
65-(12.5)80	15	45.3	1.0	0.5-0.84	1.3-2.2 $\cdot 10^6$	•	•	Mach number
115 Stator	16	16.5	3.39	0.7	1.4 $\cdot 10^6$	•	•	Incidence Mach number
Prescribed Velocity Distribution	17	35.5	1.2	0.05	1.5 $\cdot 10^5$	•	•	Incidence Mach number
EOC-7	18	48.5	1.61	0.7-0.9	7.0-10 $\cdot 10^5$	•	•	Actual velocity-density Mach number
65-(18)15 Radial Cascade	19	27.0	1.24	0.01	1.7 $\cdot 10^5$	•	•	Actual velocity-density Mach number

Note: Turbulence intensity is an additional input variable.

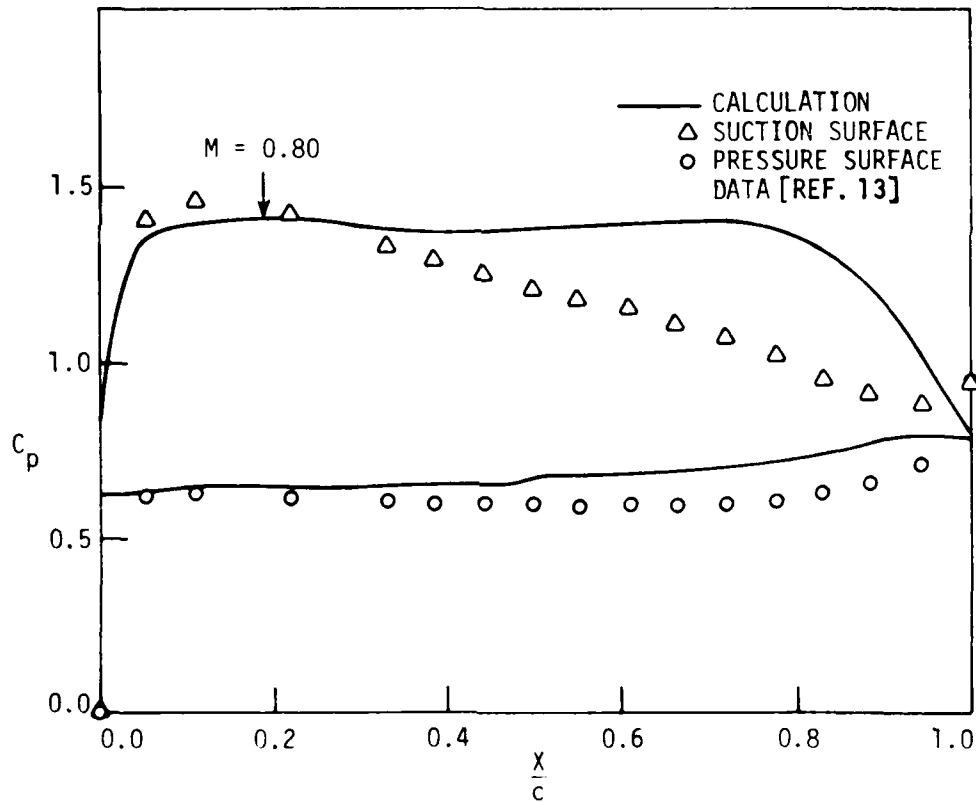
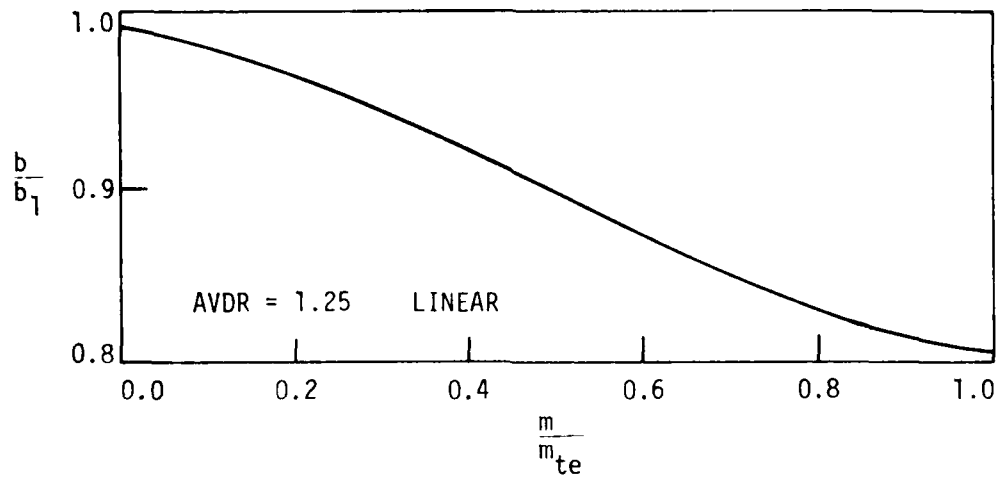


Figure 18. Calculated Surface Pressures Compared with Experimental Data for the DCA $\phi = 48^\circ$ Blade Cascade.
 $M_1 = 0.64$ $Re_c = 1.26 \times 10^6$ $\beta_1 = 40^\circ$ $i = 1^\circ$
 $D = 0.244$ $\gamma = 15^\circ$ $\sigma = 1.629$ $c = 90 \text{ mm}$

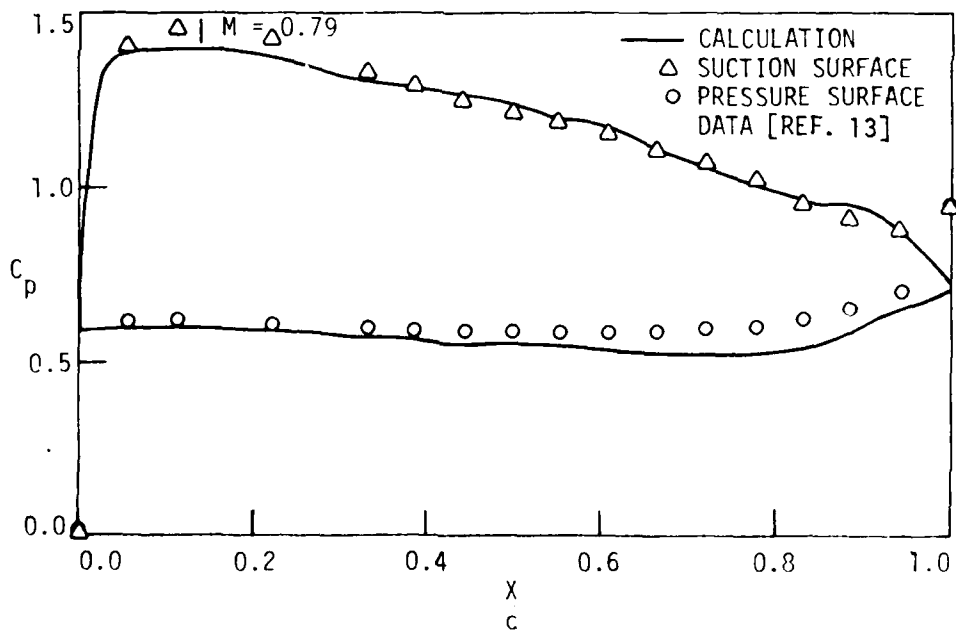
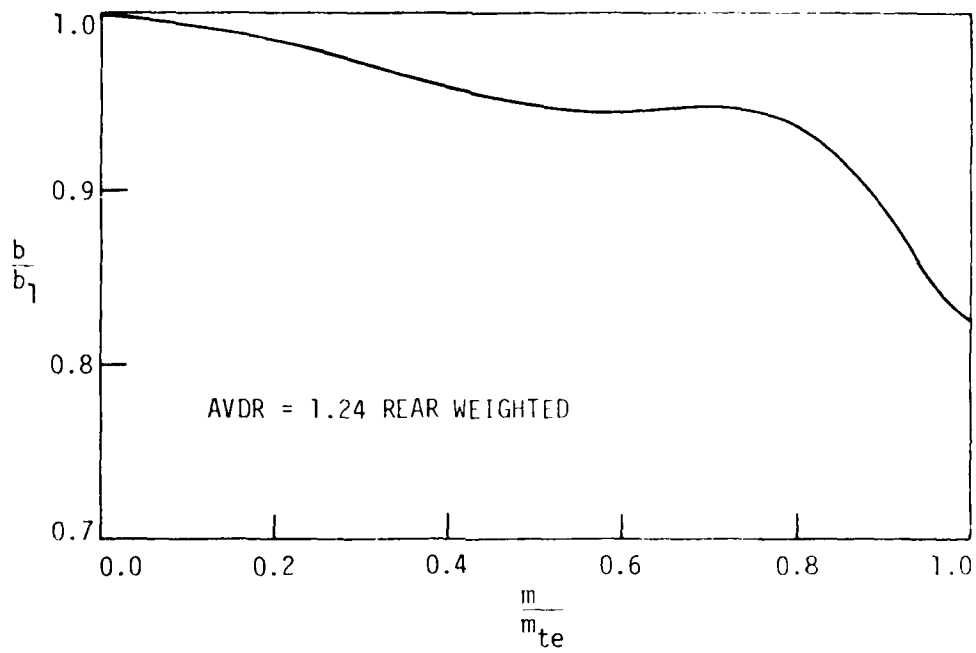


Figure 19. Calculated Surface Pressures Compared with Experimental Data for the DCA $\phi = 48^\circ$ Blade Cascade.
 $M_1 = 0.64$ $Re_c = 1.26 \times 10^6$ $\beta_1 = 40^\circ$ $i = 1^\circ$
 $D = 0.244$ $\gamma = 15^\circ$ $\sigma = 1.629$ $c = 1.24$

velocity throughout the flow field. Very satisfactory flow field comparisons between experiment and computation were reported at an inlet Mach number of 0.41 in Reference 12. At an inlet Mach number of 0.79, computed maximum flow field velocities were lower, but still favorable, when compared with the experimental measurements.

The computed flow through the 65-(12)10 cascade [Ref. 15] at low Reynolds number displays the effect of the boundary layer on direction of fluid flow (Figure 20). Computed turning at high Mach numbers did not compare favorably with the measurements, probably because axial-velocity density ratios other than 1.0 occurred in the experimental data.

The computed high-speed flow through the 65-(12A₂I_{8b})10 cascade [Ref. 15] compared well with experimental measurements. At higher Mach numbers, there was again an underestimation of the peak Mach number.

The ONERA 115 Stator cascade [Ref. 16] was the only configuration for which blade-surface boundary layer measurements were available. The comparison of the calculated boundary displacement and momentum thickness distribution with the experimental measurements was very good (Figure 21). The lack of cascade configuration boundary layer development data is an important weakness in support for computation method development and for turning angle prediction equation improvement.

The Prescribed Velocity Distribution (PVD) cascade [Ref. 17] provided a series of test cases at low Reynolds number for which the AVDR was varied at several incidence angles. These data and the corresponding computation points showed the change in the boundary layer characteristics with the variation of incidence and axial-velocity density ratio.

The LO3C-4 test cascade has considerable potential for useful results. The cascade geometry represents a cascade plane projection of a section

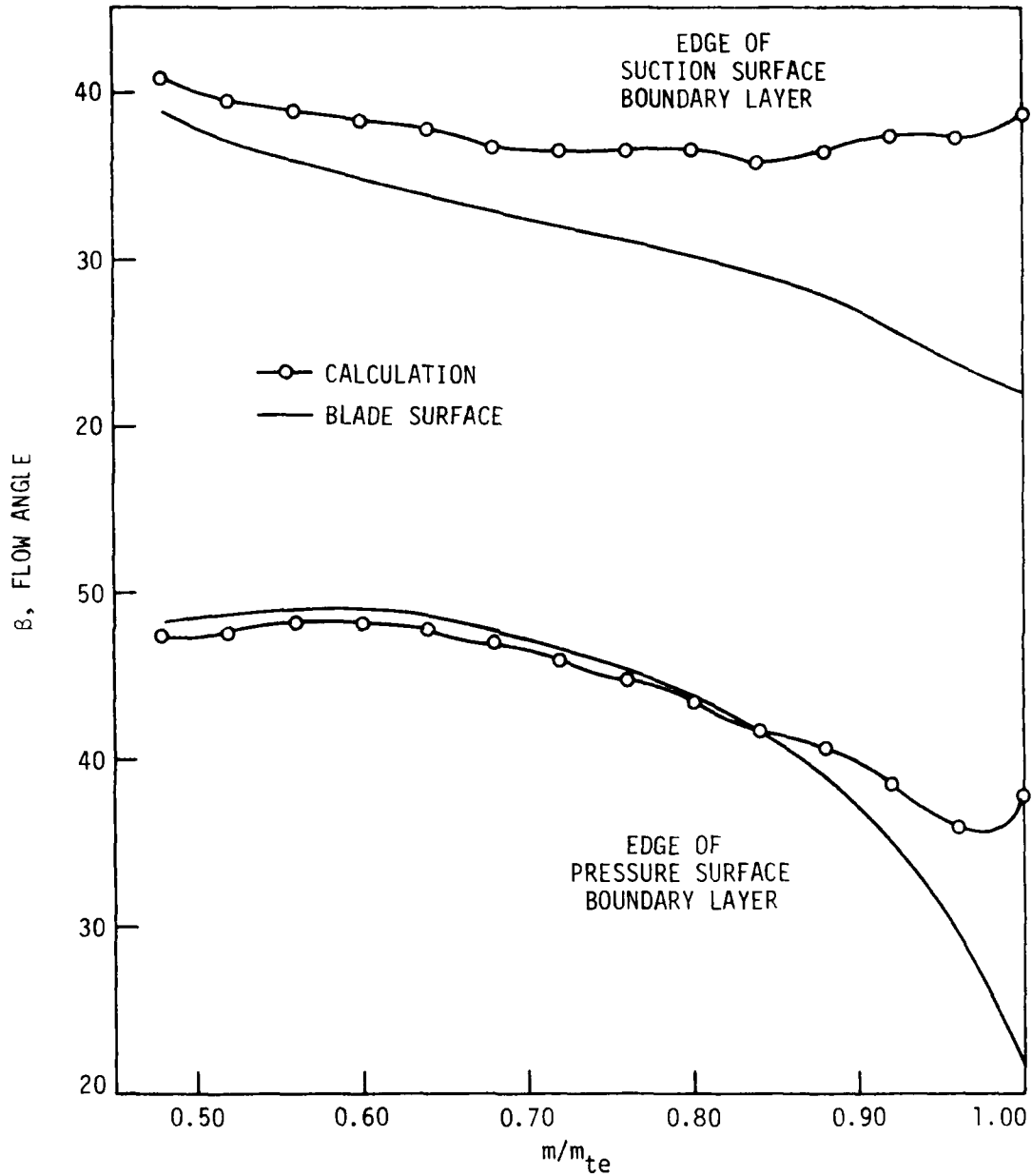


Figure 20. Calculated Flow Angle at the Edge of the Suction and Pressure Surface Boundary Layers for the NACA 65-(12)10 Blade Cascade. $M_1 = 0.06$, $Re_c = 1.47 \times 10^5$, $\beta_1 = 57.7^\circ$, $\alpha = 12^\circ$, $D = 0.42$, $\gamma = 45.7^\circ$, $\sigma = 1.0$, $c = 124$ mm, AVDR = 1.0

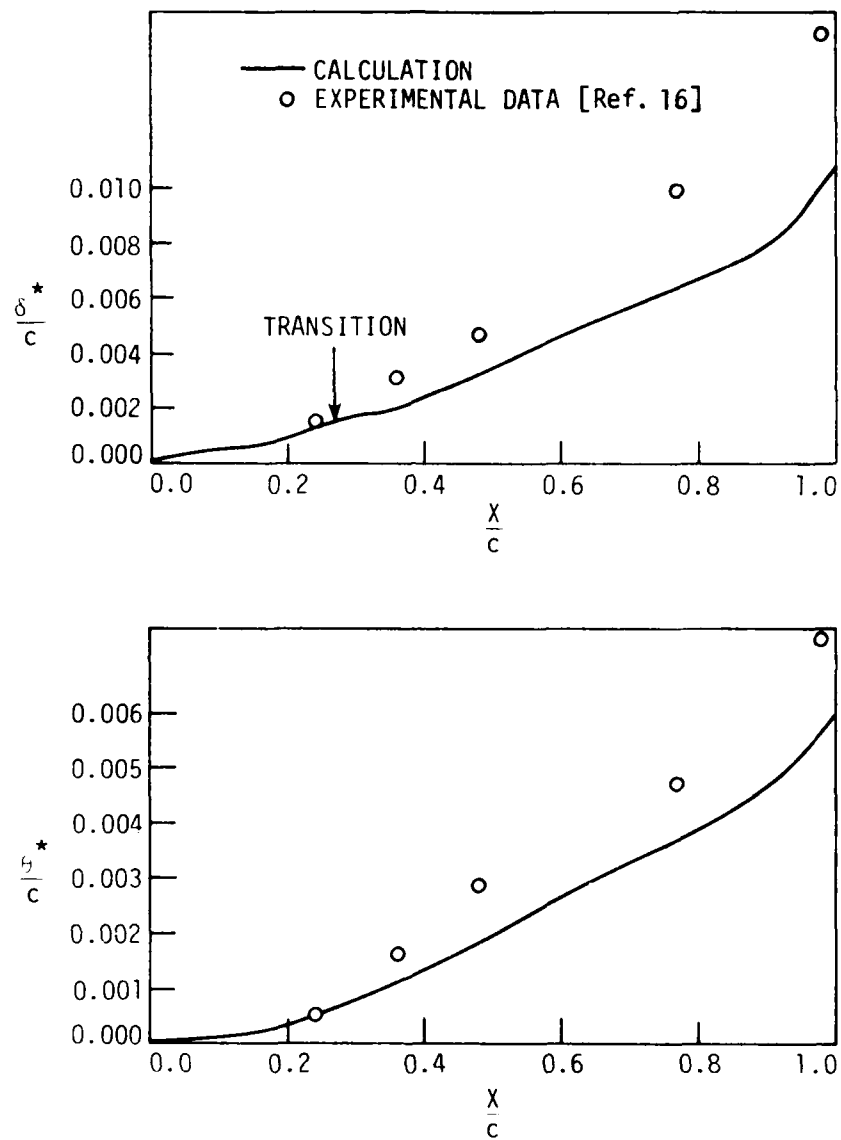


Figure 21. Calculated suction surface boundary layers compared with experimental data for the 115 stator blade cascade.

$M_1 = 0.7$ $Re_c = 1.4 \times 10^6$ $\beta_1 = 51^\circ$
 $D = 0.577$ $\gamma = 16.5^\circ$ $\sigma = 3.39$ $c = 95.6 \text{ mm}$

from the rotor of Reference 18. As a part of the test case program of AGARD Working Group 12 on Through-Flow Calculation in Turbomachines, rotor laser two-focus measurements were released along with linear cascade performance measurements. The cascade information included high Mach number turning and loss for various inlet flow angle, with one data point at the choked-flow condition. Flow field, turning and loss computation runs were completed at each of the three data points. The results have not been evaluated at this time, but will be studied in relation to other AGARD WG-12 calculations made in France and Belgium.

A NACA 65-(18)15 cascade [Ref. 19] was experimentally tested both as a radial and an axial cascade. Computations were made for both radial and axial cascade arrangements to show the effect of the radial- and axial velocity density ratio on the cascade. The results were reported in Reference 19.

4. TASK IV: EXPERIMENTAL STUDY OF MERITS OF SPECIFIC FLOW PATH GEOMETRY CHANGES IN CONTROLLING SECONDARY FLOWS IN AXIAL-FLOW COMPRESSORS

The suitability of using the existing Iowa State research compressor blading (used, for example, in Task II) for a "baseline" configuration for performance comparison with a "modified" configuration was examined at the beginning of the contract period. It was decided that a new set of baseline blades should be designed and built. Higher blade-chord Reynolds number, more suitable blade material, conventional blade section shapes, a favorable ratio of number of rotor blades to number of stator blades, and elimination of inlet guide vanes were some of the improvements expected.

The new baseline blades were designed with the aid of computer codes described in References 20 and 21. The preliminary design code [Ref. 20] is based on simple radial equilibrium of the duct flow between blade rows. A constant spanwise distribution of blade-element efficiency was involved for each blade row. For the preliminary design phase, a free-vortex swirl velocity distribution behind the rotor was used. Values of input parameters, including rotor tip and stator hub diffusion factors, rotor and stator tip axial-velocity ratios, blockage factors and rotor and stage polytropic efficiencies, were varied until reasonable input and output were achieved. The final design code [Ref. 21] is based on a streamline curvature type solution of the two-dimensional axisymmetric approximation of actual axial-flow compressor flow. It involves duct-flow stations outside blade rows. Velocity diagrams, however, are determined at blade leading and trailing edges. The code produces detailed aerodynamic, as well as blade geometry data.

The new baseline configuration consists of two identical stages as illustrated in the meridional plane sketch of Figure 22. The flow path

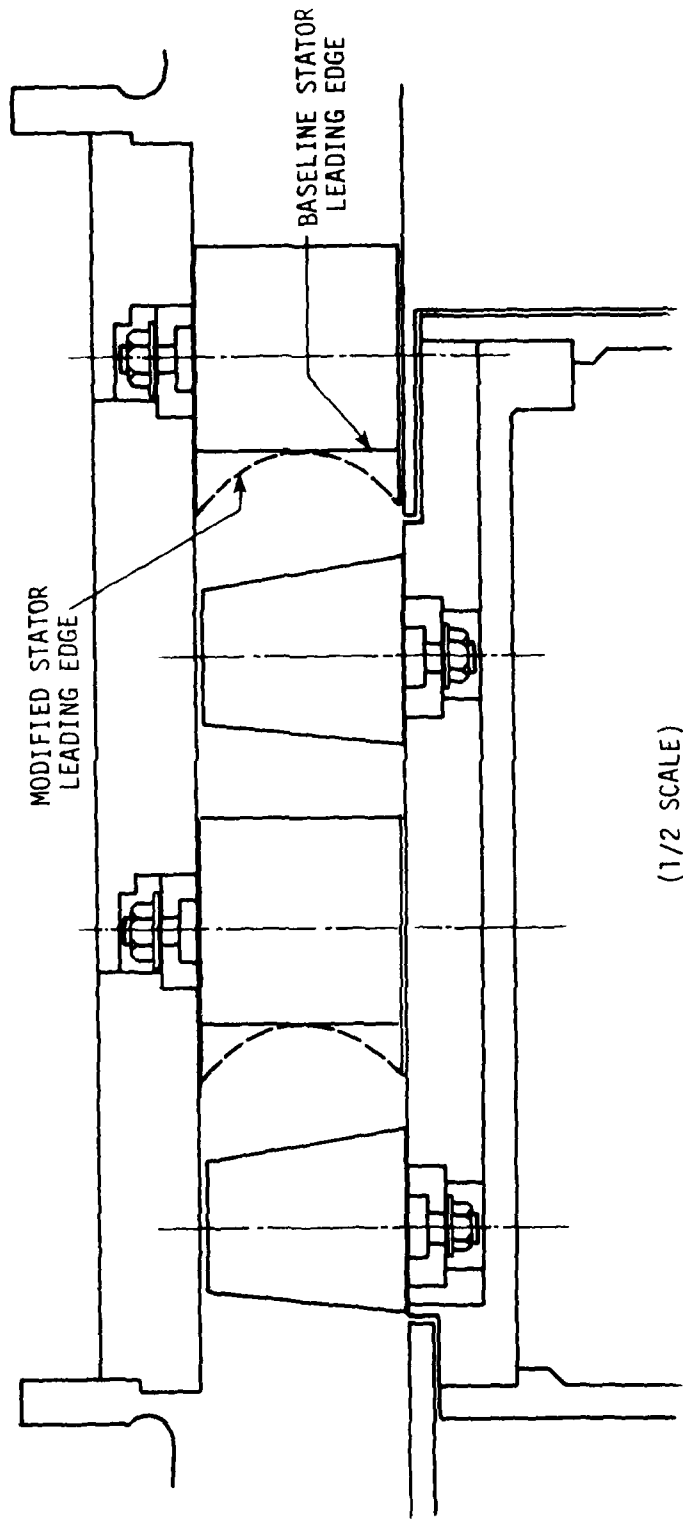


Figure 22. Meridional plane view of new blading.

dimensions involved, as well as the rotor drive system and flow rate control, are the same as before as described, for example, in Ref. 9. A summary of pertinent design data is given in Table 3. Representative blade section profiles are shown in Figures 23 and 24. Blade-element losses were approximated with values from Figure 203 of Reference 22. Blade-element incidence and deviation angles were estimated using the method proposed in Chapter VI of Reference 22. Approximate blockage factors used during the preliminary design phase were specified. Constant energy addition over the rotor span was selected.

Table 3. Summary of Baseline Compressor Design Data

Rotor speed	2400 rpm
Flow rate	5.25 lb _m /s (2.38 kg/s)
Pressure ratio	1.019
Number of blades	
Rotor	21
Stator	30
Blade material	fiberglass (steel trunnion)
Blade chord	2.39 in. (6.07 cm)
Blade profile	double circular arc
Flow path	
Hub radius	5.60 in. (14.22 cm)
Tip radius	8.00 in. (20.32 cm)

A modified stator blade with forward symmetrical sweep of the blade leading edge in the endwall regions was designed. Air Force Aero Propulsion

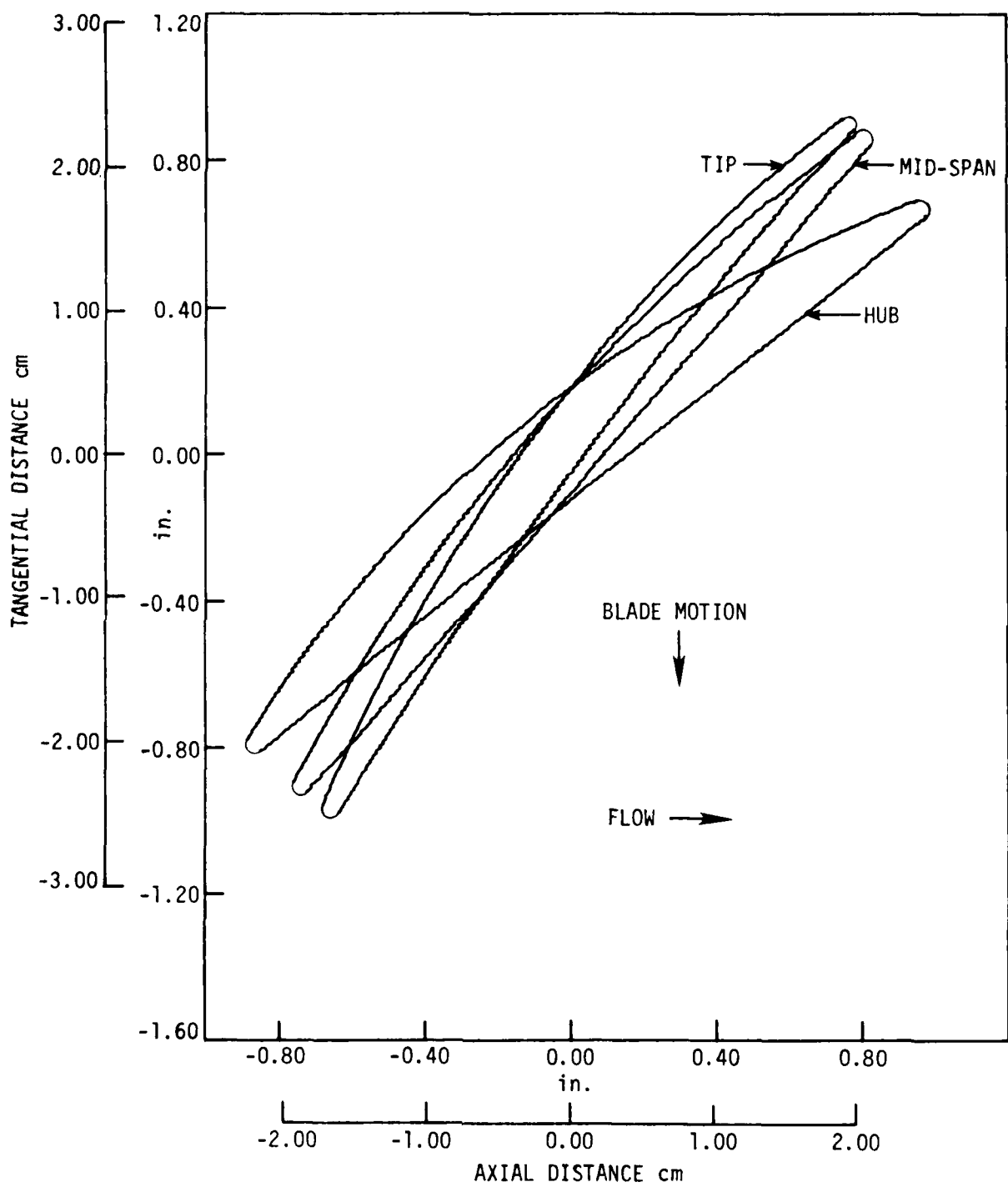


Figure 23. Representative baseline configuration rotor blade sections.

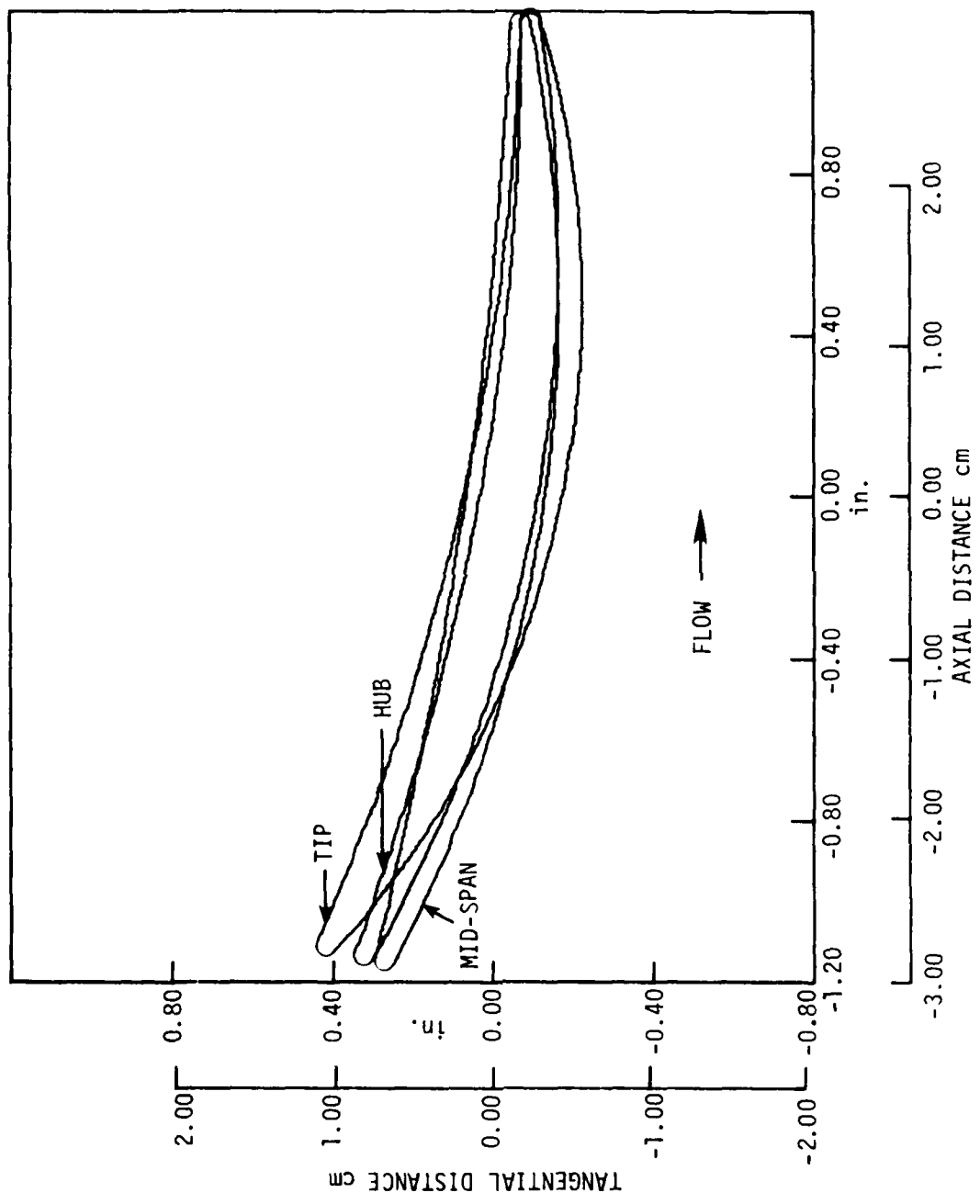


Figure 24. Representative baseline configuration stator blade sections.

Laboratory experience suggests that such a modification may lead to improved stator performance. The previously mentioned computer code [Ref. 21] was used to aerodynamically design this blade for use with the baseline rotor. Except for nonconstant chord distribution, the baseline design options were used. Some representative blade section profiles are shown in Figure 26. Because of the unusual nature of this blade, an independent analysis was made using the AFAPL UDO300 axial-flow compressor design code [Refs. 23 and 24]. Like the program in Reference 21, UDO300 employs the streamline curvature method to determine the axisymmetric approximation of the actual compressor flow. Unlike the program in Reference 21, UDO300 allows placement of calculation stations within blade rows. A comparison of incidence angles predicted by both codes for the modified blade configuration designed with the code of Ref. 21 is shown in Figure 26. Since the incidence angles were similar, it was decided that the modified blade configuration designed with the NASA code was suitable for use.

Performance testing of the baseline compressor is scheduled to begin in late 1980 and will consist mainly of time-average and periodic-average total-pressure and flow velocity measurements. Design-point operation flow field properties will be ascertained in detail. Some off-design data, such as the rotating stall limit, will be acquired. The baseline configuration blades have been fabricated and have been mounted on the rotor hub and stator rings. Blade tip clearances are being machined and the baseline compressor testing should commence in December 1980. Eyelash gage checks of the blade profiles indicate very good correspondence with the design coordinates.

Testing of the modified compressor is anticipated to begin in 1981. Fabrication of the modified stator blades will begin soon; the contract

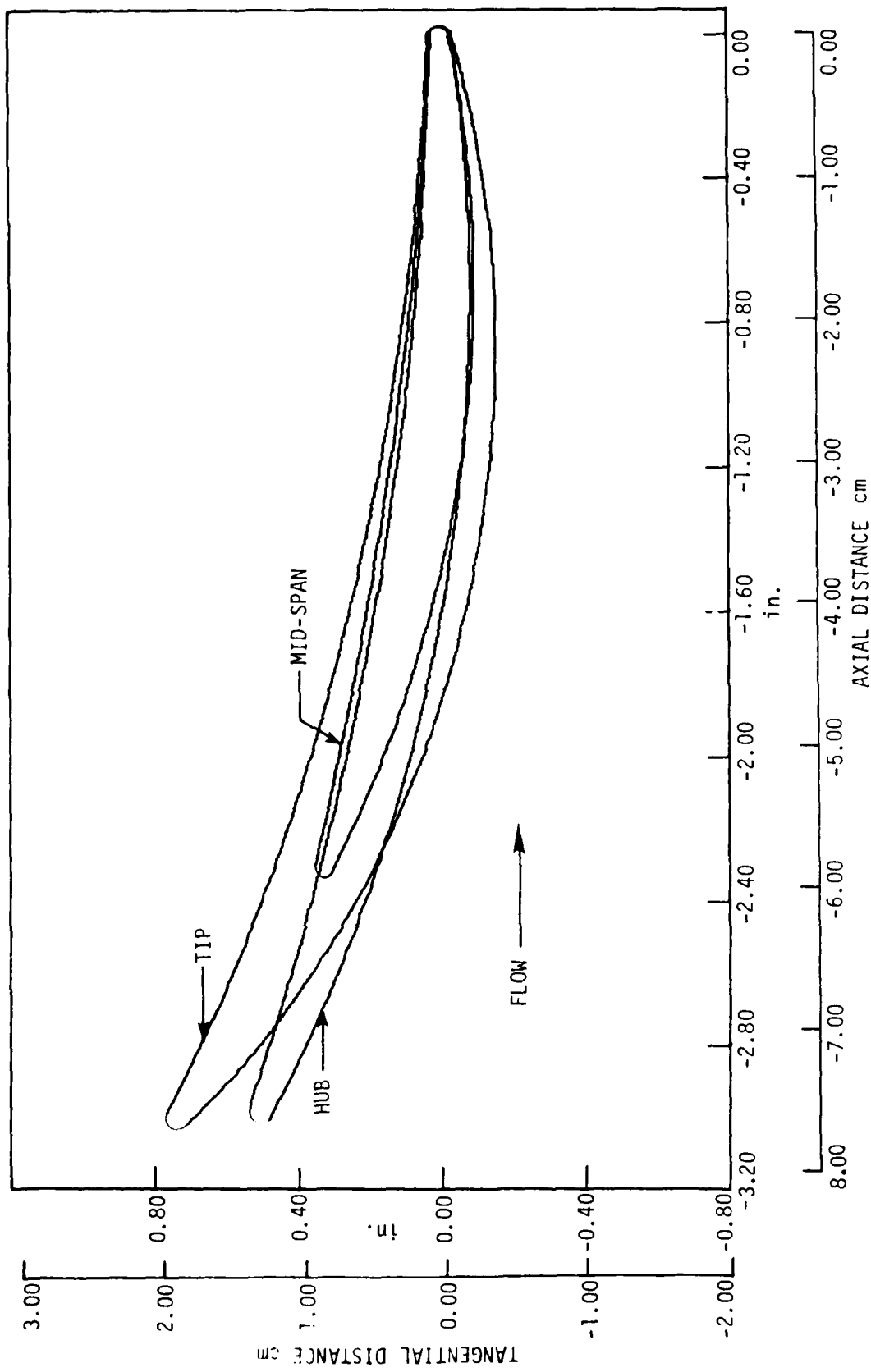


Figure 25. Representative modified stator blade sections.

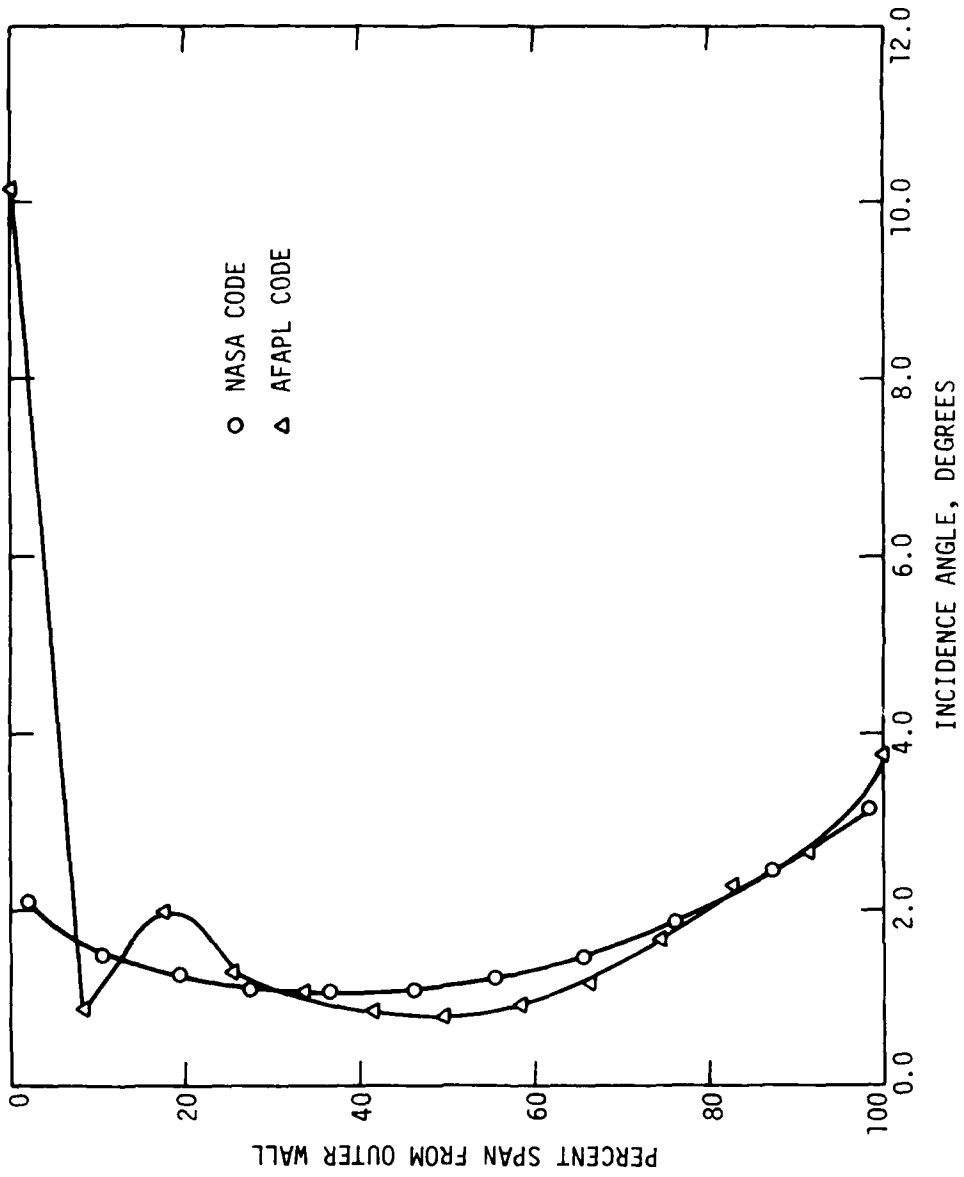


Figure 26. Comparison of modified stator leading edge incidence angle predictions calculated using different compressor design computer codes.

involved has been awarded. Time-average and periodic-average total-pressure and flow velocity measurements for design-point and off-design operation will be acquired and compared with baseline results.

5. TASK V: DEFINITION OF EXPERIMENTAL PROGRAMS AND FACILITIES APPROPRIATE FOR UNIVERSITY TURBOMACHINERY RESEARCH PROGRAMS

A very wide range of research and development activity is currently carried on in the field of turbomachine aerodynamics. This research and development takes place in all highly-industrialized countries of the world, and in a few countries that are less developed. Some characteristics of turbomachinery research, as distinguished from development, should be recognized:

1. In the United States, for many years, the position was taken in important elements of the aircraft propulsion and industrial turbomachinery industries that, because of the "proprietary" nature of the information generated in turbomachinery-related experiments, turbomachine aerodynamic research was industrial business and not appropriate for university programs. To a lesser degree, and for slightly different reasons, some government research funding agencies took the same point of view. To some extent, this attitude exists today.
2. In the remainder of the world, a different view exists. Every country which is technically competitive with the United States has from two to several active university research programs in turbomachinery fluid dynamics, usually in a formally organized and supported institute or laboratory with a Professor as director, and a technical staff.
3. The facilities available to university turbomachinery research groups in the United States are modest, marginal or inadequate. A number of "apparent" research programs are largely based on work generated through industrial consulting or on data supplied from government laboratory in-house experiments.

4. Turbomachinery experimental facilities in European and Japanese universities are custom-designed and highly appropriate for continuing research. Most are comparable in quality to industrial and government research laboratory facilities in the United States.

Some turbomachinery aerodynamic research should not be carried on in universities. Prohibitive facility operating cost and safety considerations might be typical reasons for disqualification of some classes of research. However, there are several categories of research projects which can be considered as well-matched to university characteristics, including faculty qualifications, student capability and available support services. Three are outlined in Sections 5.1 to 5.3.

5.1. Experiments in Low-Speed Rotating Test Facilities

Performance significant aerodynamic phenomena in fan, compressor and turbine flow path components can be effectively studied in low-rotational-speed test units. At moderate to large scale, useful detailed measurements can be made at moderate to low cost.

Secondary flows and geometrical means for modifying or controlling secondary flows remain an unresolved problem area in axial and centrifugal compressors and turbines. The careful definition of three-dimensional effects by measurements is necessary to permit design improvements and also to produce test or "benchmark" data for development of computational methods. Present availability of such data is totally inadequate and new ideas are genuinely needed.

The widespread significance of the essential unsteadiness in turbomachinery flows has become increasingly evident. Although useful work has been done in university turbomachinery research facilities in exposing

important features of unsteady flows in compressors and turbines, a great deal of quantitative evaluation remains to be done. This type of investigation is being carried on in aircraft engine industry laboratories, but additional large-scale, low-speed facilities could be utilized without overcrowding the field. The patient and original work of advanced students would be a valuable asset in both experimentation and data analysis.

Nearly all current low-speed compressor and turbine test facilities are single-stage configurations. Both the unsteady and secondary flow effects should also be studied in multistage environments. A multistage test unit could be efficiently and economically operated for research purposes in a university.

5.2. Experiments in Linear Cascade Facilities

The computational study carried out under Task III of the present program demonstrated clearly that there is insufficient information available on the flow fields found in linear airfoil cascades. To permit development of more satisfactory turning and loss prediction systems for compressor and turbine cascade flows, a carefully laid out sequence of test case data points should be made available. There are only a few linear cascade facilities now operational in the United States. Only one approaching test case quality exists in a university. This contrasts greatly with the situation in Europe where graduate student research in cascade facilities has generated a substantial fraction of the cascade flow field information available in the world today.

5.3. Experiments Evaluating and Introducing New or Improved Measuring Techniques

A third class of research suited to university programs is the development of non-traditional instrumentation and measurements systems for

turbomachinery flows. Detailed flow field mapping, and measurements in unsteady turbomachine flows are manpower-intensive research activities. Universities now engaged in turbomachinery experimentation have been especially successful in the introduction of new measurement techniques. The scope of typical projects in measurement methods is such that individual problems can be isolated and attacked readily by faculty-student groups.

SECTION III

PUBLICATIONS

The following list includes documents based entirely, or in part, on research supported under the current contract.

1. Hansen, E. C., Serovy, G. K., and Sockol, P. M. Axial-Flow Compressor Turning Angle and Loss by Inviscid-Viscous Interaction Blade-to-Blade Computation. *Journal of Engineering for Power*, Trans. ASME. 102: 28-34. 1980.
2. Hansen, E. C., Serovy, G. K., and Sockol, P. M. Axial-Flow Compressor Turning Angle and Loss by Inviscid-Viscous Interaction Blade-to-Blade Computation. NASA Technical Note, in review process.
3. Hottman, D. A. Turbomachinery Laboratory Data Acquisition and Experiment Control System. To be published as Iowa State University Engineering Research Institute Technical Report TCRL-19. 1980.
4. Kavanagh, P. The Stuart and Hetherington Numerical Solution Method for Three-Dimensional Compressible Internal Flows. Engineering Research Institute Report. ISU-ERI-Ames-78310, TCRI-12. Iowa State University, Ames, Iowa. 1978.
5. Morgan, Betsy D. A Water Column Balance Pressure Reference System. Turbomachinery Components Research Program. Unpublished report. Department of Mechanical Engineering. Iowa State University, Ames, Iowa. 1979.
6. Okiishi, T. H. Turbomachine Wake Transport and Interaction. In von Karman Institute for Fluid Dynamics Lecture Series Unsteady Flow in Turbomachines Notes. Rhode-St.-Genèse, Belgium. 1979.

7. Okiishi, T. H. Some Fundamental Unsteady Flow Measurements in Turbomachines. In University of Tennessee Space Institute Lecture Series Flow Induced Vibration Problems and Their Solutions in Practical Applications: Turbomachinery, Heat Exchangers and Nuclear Reactors Notes. Tullahoma, Tennessee. 1979.
8. Okiishi, T. H., and Schmidt, D. P. Measurement of the Periodic Variation of Turbomachine Flow Fields. In Proceedings of the Dynamic Flow Conference 1978 on Dynamic Measurements in Unsteady Flows. Proceedings of the Dynamic Flow Conference 1978. Skovlunde, Denmark. 1979.
9. Okiishi, T. H. Periodically Unsteady Flow Through an Imbedded Stage of a Multistage Axial-Flow Turbomachine. In Aeroelasticity of Turbine Engines, Joint NASA/AF/Navy Symposium Preprint. October 1980.
10. Serovy, G. K., and Hansen, E. C. Computation of Flow in Radial- and Mixed-Flow Cascades by an Inviscid-Viscous Interaction Method. In Centrifugal Compressors, Flow Phenomena and Performance. AGARD-CP-282. 1980.
11. Serovy, G. K. Deviation/Turning Angle Correlations. To be published in Final Report of AGARD/PEP Working Group 12 on Through Flow Calculations in Turbomachines.
12. Serovy, G. K. Axial-Flow Turbomachine Through-Flow Calculation Methods. To be published in Final Report of AGARD/PEP Working Group 12 on Through Flow Calculations in Turbomachines.
13. Smith, P. Flow Calibration of Five-Hole Directional Pressure Probes. To be published as Iowa State University Engineering Research Institute Technical Report TCRL-20. 1980.

14. Zierke, W. C., and Okiishi, T. H. Measurement and Analysis of the Periodic Variation of Total Pressure in an Axial-Flow Compressor Stage. To be published as an Iowa State University Engineering Research Institute Technical Report TCRL-18. December 1980.

SECTION IV
PROGRAM PERSONNEL

Three principal investigators share responsibility for the current program.

- George K. Serovy, Anson Marston Distinguished Professor in
Engineering, Tasks III, IV, V
- Patrick Kavanagh, Professor of Mechanical Engineering, Task I
- Theodore H. Okiishi, Professor of Mechanical Engineering, Tasks II,
IV

Four graduate-level engineers were also associated with the work.

- John A. McAndrew, Graduate Research Assistant, Task I
- Elmer C. Hansen, Post-Doctoral Research Fellow (to 1 October 1979),
Tasks III, IV
- William C. Zierke, Graduate Research Assistant, Task II
- Michael D. Hathaway, Graduate Research Assistant, Task IV

During the research, several undergraduate students in Mechanical Engineering made useful contributions. This was an effective mechanism for introducing undergraduates to the research activity in turbomachinery.

- Mark T. Diefenthaler, Undergraduate Assistant, Task I
- Allen D. Dvorak, Undergraduate Assistant (to 1 June 1980), Task I
- Douglas A. Hottman, Undergraduate Assistant, Task I
- J. Scott Meline, Undergraduate Assistant (to 1 June 1979), Task I
- Betsy D. Morgan, Undergraduate Assistant (to 1 June 1979), Task I
- Brian H. Pigg, Undergraduate Assistant (to 1 June 1979), Task I
- Paul G. Smith, Undergraduate Assistant, Task I

SECTION V

INTERACTION WITH FEDERAL AGENCIES AND INDUSTRY

The turbomachinery research program at Iowa State University has focused on projects which make a contribution to the development of design systems for advanced compressors, fans, and turbines for air-breathing aircraft propulsion systems. The current contract has not changed this focus and has involved numerous direct contacts with outside organizations.

Task II is a continuation of turbomachine unsteady flow measurement work initiated under AFOSR Grant 76-2916. Related interactions involving formal written discussions and informal conversations about measurement techniques and data are summarized below.

Organization and Nature of Contact

Individual Contacts

von Karman Institute for Fluid Dynamics,
Rhode-St.-Genèse, Belgium; formal lectures,
lab visit, other technical discussions

F.A.E. Breugelmans

Institut für Strahlantriebe und
Turboarbeitsmaschinen, Technische
Hochschule, Aachen, West Germany; lab
visit and technical discussions, review
of technical paper

H. E. Gallus

Turbopropulsion Laboratory, Department of
Aeronautics, Naval Post-graduate School,
Monterey, California; formal lecture, lab
visit, and technical discussions

R. P. Shreeve

NASA-Lewis Research Center, Cleveland Ohio; lab visits and technical discussions	C. Ball M. Hartmann A. J. Strazisar
The Trane Company, LaCrosse, Wisconsin; telecom technical discussions	D. B. Schmidt
United Technologies Research Center, East Hartford, Connecticut; telecom technical discussions	J. H. Wagner
Department of Civil and Mechanical Engineering, University of Tasmania, Hobart, Tasmania; technical discussions	G. J. Walker
Department of Aerospace Engineering, Pennsylvania State University, University Park, Pennsylvania; technical exchange of data, formal discussion of research	B. Lakshminarayana
University of Tennessee Space Institute, Tullahoma, Tennessee; formal lecture	M. Kurosaka J. E. Caruthers

Task III has involved use of experimental test cases selected to demonstrate capabilities and limitations of the cascade flow field computation system. It has also involved continued cooperation with the initial sponsors at the NASA-Lewis Research Center. Mr. M. J. Hartmann, Chief, Fluid System Component Division, Lewis Research Center, has approved use of the NASA computation facilities for test case examples.

Organization and Nature of Contact

Individual Contacts

Air Research, Phoenix Division, Phoenix,
Arizona; test cases

J. R. Switzer

Institut für Antriebstechnik, Deutsche
Forschungs- und Versuchsanstalt für Luft-
und Raumfahrt, Köln, West Germany; test
cases, review of results

Dr. G. Winterfield

Dr. H. Starcken

Dr. J. Renken

Dr. H. B. Weyer

Direction de l'Energetique, Office National
d'Etudes et de Recherches Aérospatiales,
Châtillon-sous-Bagneux, France; test cases,
review of results

J. Fabri

G. Meauzé

NASA-Lewis Research Center, Cleveland,
Ohio; computation, test cases, review
of results

M. J. Hartmann

P. M. Sockol

D. M. Sandercock

J. F. Schmidt

J. Wood

Task IV depends on substantial cooperation with USAF/AFAPL and industry.

A list of the visits and telephone contacts for Task IV follows.

Organization and Nature of Contact

Individual Contacts

NASA-Lewis Research Center, Cleveland,
Ohio; exchange of computer programs,
review of designs

D. M. Sandercock

J. E. Crouse

Air Force Aero Propulsion Laboratory,
Wright-Patterson Air Force Base, Ohio;
discussion and review of designs for
base and modified stages

Dr. A. J. Wennerstrom
Dr. C. Herbert Law

General Electric Company, Advanced Turbo-
machinery Aerodynamics, Cincinnati, Ohio;
review of design

Dr. D. C. Wisler
Dr. L. H. Smith, Jr.

Pratt & Whitney, East Hartford, Connecticut;
discussion of blade fabrication problems

H. Weingold
A. W. Stubner

SECTION VI

DISCOVERIES, INVENTIONS AND SCIENTIFIC APPLICATIONS

No fundamentally new concepts or devices were developed. However, Task IV involves some blade design concepts which originated in AFAPL and may, after experimental evaluation and development, lead to improved multi-stage compressor performance.

SECTION VII

CONCLUDING REMARKS

During a two-year contract period, the program objectives supported by USAF/AFOSR F49620-79-C-0002 have been realized. A test installation for generation of detailed flow field data in curved-mean-line, rectangular cross-section passages has been built, instrumented and calibrated. A coordinated set of computational and experimental test cases is being accumulated (Task I). New data on unsteady blade-row interactions in a multistage compressor environment have been measured, reduced and evaluated. These data are expected to lead to the introduction of mechanisms for unsteady flow accounting in compressor design (Task II). A broad range of computational test cases, involving direct prediction of airfoil cascade turning, loss and internal flow field for compressor cascade arrangements, was completed. These test case results, when compared with corresponding experimental data from linear cascades, show that an inviscid-viscous interaction method is capable of producing realistic values. Predicted loss and turning can be used to study trends produced by changes in most of those cascade aerodynamic variables that are significant in current compressor design (Task III). In a continuing project concerned with evaluation of means for control of secondary flow losses in multistage axial-flow compressors, two two-stage configurations were designed, a base or reference geometry and a secondary flow control stator geometry. The first two-stage blading set was built and is being installed in preparation for the test program (Task IV). A study was made to recommend classes of experimental projects which could contribute data useful to designers and developers of advanced compressors and turbines, and which could be

reasonably matched to the facility and personnel characteristics of university laboratories. Three classes of experiments are suggested in this report (Task V).

The program in AERODYNAMICS OF ADVANCED AXIAL-FLOW TURBOMACHINERY has been technically successful. In addition it has directed the attention of a significant number of undergraduate and graduate students toward the objectives of current research in a field of aerodynamics which has not received adequate emphasis in government-university programs. Direct association and cooperation between the aircraft propulsion industry, USAF and NASA laboratories, faculty and students will assist in the maintenance of United States technological quality in air-breathing aeronautical propulsion.

SYMBOLS AND NOTATION

AVDR	ratio of blade row exit to entrance axial velocity \times density product
b	blade-to-blade streamsheet thickness
b_1	blade-to-blade streamsheet thickness at cascade entrance
C_p	pressure coefficient
c	blade chord length
D	diffusion parameter [Ref. 22]
HT	total head
i	incidence angle
M	Mach number
M_i, M_1	cascade entrance Mach number
m	meridional distance measured from row leading edge
m_{te}	meridional distance to trailing edge
PHH	percent passage height from hub
Re_c	Reynolds number based on chord length
S_S	circumferential distance between two adjacent stator blades
S_R	circumferential distance between two adjacent rotor blades
X	distance along chord line
Y	circumferential distance from the reference meridional plane to the measurement point
YO_{IGV}	circumferential distance from the reference meridional plane to the reference IGV blade stacking axis
YO_{1S}	circumferential distance from the reference meridional plane to the reference first stator row blade stacking axis
YO_R	circumferential distance from the reference meridional plane to the reference first rotor row blade stacking axis

α	angle of attack
β	local flow angle measured from axial direction
β_1	inlet flow angle measured from axial direction
γ	blade setting angle
δ^*	boundary layer displacement thickness
θ^*	boundary layer momentum thickness
σ	solidity
ϕ	blade camber

REFERENCES

1. Hottman, D. A. Turbomachinery Laboratory Data Acquisition and Experiments Control System. Rep. TCRL-19, Turbomachinery Components Research Program, Department of Mechanical Engineering and Engineering Research Institute, Iowa State University, Ames, Iowa. 1980.
2. Morgan, Betsy D. A Water Column Balance Pressure Reference System. Turbomachinery Components Research Program. Unpublished Report. Department of Mechanical Engineering, Iowa State University, Ames, Iowa. 1979.
3. Smith, P. G. Calibration of Five-Hole Directional Pressure Probes. Rep. TCRL-20, Turbomachinery Components Research Program, Department of Mechanical Engineering and Engineering Research Institute, Iowa State University, Ames, Iowa. 1980.
4. Kernighan, B. W. UNIX for Beginners. Bell Laboratories, Murray Hill, N.J. 1972.
5. Camarata, F. J., Hooper, R. M., and Nice, M. L. Experimental Investigation of Passage Flow in Baseline Build of Large-Scale Turbine Cascade. Rep. R75-212632, United Aircraft Research Laboratories, E. Hartford, Conn. 1975.
6. Langston, L. S., Nice, M. L. and Hooper, R. M. Three-Dimensional Flow Within a Turbine Cascade Passage. ASME Paper No. 76-GT-50. 1976.
7. Okiishi, T. H. "Turbomachine Wake Transport and Interaction." In von Karman Institute for Fluid Dynamics Lecture Series: Unsteady Flow in Turbomachines Notes. Rhode-St.-Genèse, Belgium. 1979.
8. Zierke, W. C. and Okiishi, T. H. Measurement and Analysis of the Periodic Variation of Total Pressure in an Axial-Flow Compressor Stage. Rep. TCRL-18, Turbomachinery Components Research Program, Department of Mechanical Engineering and Engineering Research Institute, Iowa State University, Ames, Iowa. 1980.
9. Wagner, J. H., Okiishi, T. H. and Holbrook, G. J. Periodically Unsteady Flow in an Imbedded Stage of a Multistage, Axial-Flow Turbomachine. Trans. ASME. Jour. of Engr. for Power, 101: 42-51. 1979.
10. Serovy, G. K. Deviation Angle/Turning Angle Prediction for Advanced Axial-Flow Compressor Blade Row Geometries. Final Report. USAF/AFAPL Contract F33615-76-C-2090. AFAPL-TR-77-81. 1978.

11. Hansen, E. C. Blade-Surface Boundary Layer and Wake Computational Models for Estimation of Axial Flow Compressor and Fan Blade-Row Deviation Angles and Losses. Unpublished Ph.D. Dissertation. Iowa State University, Ames, Iowa. 1978.
12. Hansen, E. C., Serovy, G. K. and Sockol, P. M. Axial-Flow Compressor Turning Angle and Loss by Inviscid-Viscous Interaction Blade-to-Blade Computation. Trans. ASME. Jour. of Engr. for Power, 102: 28-34. 1980.
13. Starcken, H., Breugelmans, F. A. E., and Schimming, P. Investigation of the Axial-Velocity Density Ratio in a High Turning Cascade. ASME Paper No. 75-GT-25. 1975.
14. Bunimovich, A. I., and Svyatogorov, A. A. "Aerodynamic Characteristics of Foil Compressor Cascades at High Subsonic Speeds." FTD-MT-24-69-68. April 26, 1968. Translation of "Lopatochnyye Mashiny i Struynyye Apparaty." Sbornik Statey. Vypusk 2. Moscow. Izdatel'stvo Mashinostroyeniye. 1967. pp. 5-35.
15. Dunavant, J. C., Emery, J. C., Walch, H. C., and Westphal, W. R. High Speed Cascade Tests of the NACA 65-(12A₁₀)10 and NACA 65-(12A₂I_{8b})10 Compressor Blade Sections. U.S. NACA RM L55108. 1955.
16. Meauzé, G. Transonic Boundary Layer on Compressor Stator Blades as Calculated and Measured in Wind Tunnel. Paper given at International Symposium on Air Breathing Engines IV. 1979.
17. Masek, Z., and Norbury, J. F. "Low-Speed Performance of a Compressor Cascade Designed for Prescribed Velocity Distribution and Tested with Variable Axial Velocity Ratio. In Heat and Fluid Flow in Steam and Gas Turbine Plant. IME Conference Publication 3. 1973. pp. 276-287.
18. Dunker, R. J., and Hungenberg, H. G. Transonic Axial Compressor Using Laser Anemometry and Unsteady Pressure Measurements. AIAA Journal 18: 973-979. 1980.
19. Serovy, G. K., and Hansen, E. C. Computation of Flow in Radial- and Mixed-Flow Cascades by an Inviscid-Viscous Interaction Method. In Centrifugal Compressors, Flow Phenomena and Performance. AGARD-CP-282. 1980.
20. Bryans, A. C., and Miller, M. L. Computer Program for Design of Multistage Axial-Flow Compressors. U.S. NASA CR-54530. Allison EDR-4575. 1967.
21. Crouse, J. E. Personal communication. 1978.

22. Johnson, I. A., and Bullock, R. O., eds. Aerodynamic Design of Axial-Flow Compressors. U.S. NASA SP-36. 1965.
23. Hearsey, R. M. A Revised Computer Program for Axial Compressor Design Volume 1: Theory, Descriptions and User's Instructions. ARL TR 75-0001 Volume 1. Aerospace Research Laboratories, Wright-Patterson Air Force Base, Ohio, 1975.
24. Hearsey, R. M. Revised Computer Program for Axial Compressor Design Volume 2: Program Listing and Program Use Example. ARL TR 75-0001 Volume 2. Aerospace Research Laboratories, Wright-Patterson Air Force Base, Ohio, 1975.

APPENDIX A

EXPERIMENTAL DATA TABULATION FOR PASSAGE TEST RIG, TASK I

Sample data tables, representative of how data are collected by the data acquisition system and stored on disk, are shown and discussed. Three data tables are presented:

- (1) Five-hole probe as-measured traverse pressures and recorded temperatures for a given traverse plane and slide bar position.
- (2) First-pass reduced data based on probe calibration curves (Ref. 4).
- (3) Sidewall and endwall static pressures for given traverse plane, and reference pitot pressures at midpoint of entering boundary layer to test section.

The first two tables indicate five-hole probe data for a given "pass" of the probe for various Z-positions between the endwalls of the passage. Probe position in the passage is recorded by the label in the right-most column of these tables. This label also serves as file identification for the line of data in the table as stored.

In the third table, static taps 1-16 are those in the suction sidewall for the given traverse plane; the taps are spaced at 1-inch intervals with tap No. 1 located 0.5 inch below the upper endwall. Likewise, 17-32 are in the pressure sidewall, with No. 17 located 0.5 inch below the upper endwall. For static pressures along the endwall, obtained with the static tap fixture installed in the slide bar, the x-position of the tap is recorded with the associated pressure measurement.

Definitions of measured and reduced data terms are listed below (see also Fig. A1 for passage dimensions, coordinate system and slide bar numbers):

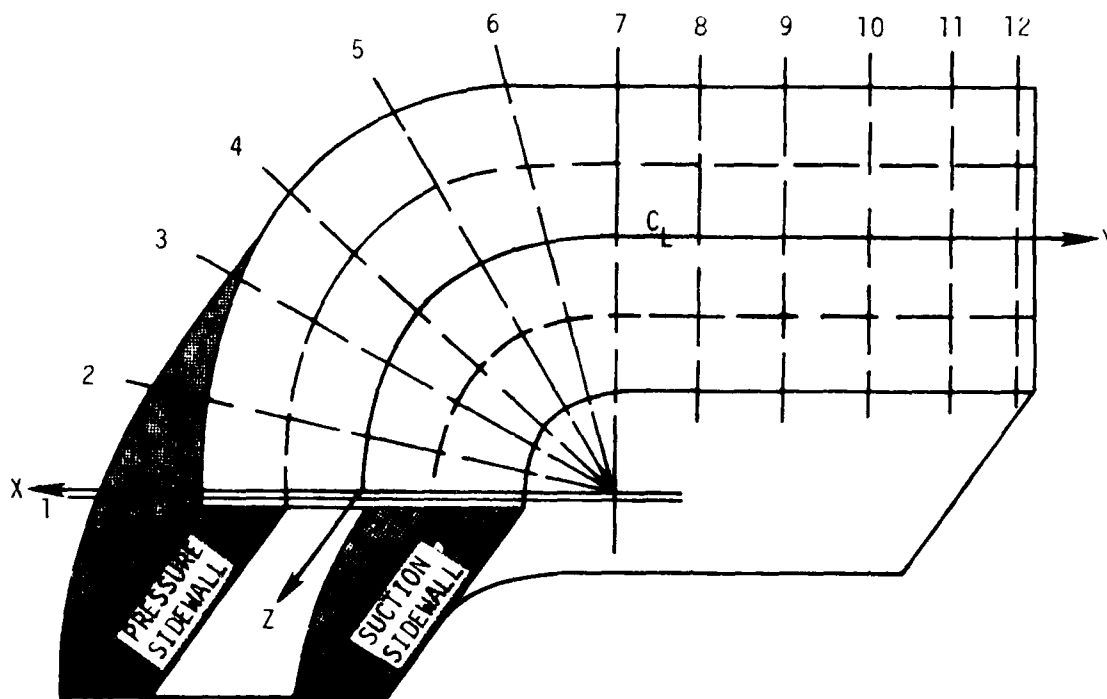
ATM	atmospheric (reference) pressure, in H ₂ O
PO	plenum (reference) pressure, in H ₂ O
P1,P4,P5	five-hole probe impact and pitch pressures
PBAR	barometric pressure, in Hg (abs)
PITCH	pitch angle (deg determined from probe calibration)
POS	position of five-hole probe (three numbers, separated by percent signs, are used indicating x, slide bar No., and Z, respectively. Values of x when negative are prefixed by the letter M)
PSO	pitot static pressure, in H ₂ O (gage)
PT	total pressure, from probe calibration, in H ₂ O (gage)
Q	dynamic pressure, from probe calibration
QO	pitot dynamic pressure, in H ₂ O
TBAR	atmospheric temperature, deg F
TPLEN	plenum temperature, deg F or deg R
VEL	velocity V, ft/s (see reduction formula below)
YAW	measured yaw angle (determined by probe null) from reference yaw for test section; yaw angle corrected for pitch (from probe calibration)

Data reductions from the tabulated data are as follows:

- (1) Total pressure coefficient, C_{pt} , is defined as

$$C_{pt} = (p_{to} - p_t) / q_o$$

where p_t is total pressure, and p_{to} , q_o are reference pitot total and dynamic pressures, respectively. Based on table entries, then,



TRAVERSE PLANE No.	Y, INCHES(cm)	PASSAGE WIDTH INCHES, (cm)
1 (INLET)	-0.500 (-1.27)	9.00 (22.86)
2 (15 deg)	5.498 (13.97)	9.00 (22.86)
3 (30 deg)	10.996 (27.94)	8.80 (22.35)
4 (45 deg)	16.493 (41.89)	8.48 (21.54)
5 (60 deg)	21.991 (55.86)	8.00 (20.32)
6 (75 deg)	27.489 (69.82)	7.80 (19.81)
7 (90 deg)	32.987 (83.79)	7.80 (19.81)
8 (DISCHARGE)	38.487 (87.60)	7.75 (19.69)
9 (DISCHARGE)	43.987 (110.46)	7.75 (19.69)
10 (DISCHARGE)	49.487 (125.70)	7.75 (19.69)
11 (DISCHARGE)	54.987 (138.40)	7.75 (19.69)
12 (DISCHARGE)	60.487 (153.64)	7.75 (19.69)

Figure A1. Schematic of test section showing dimensions, traverse plane identification and coordinate system convention.

$$C_{pt} = 1 - (PT/QO) + (PS/QO)$$

(2) Static pressure coefficient, C_{ps} , is defined as

$$C_{ps} = (p_s - p_{so})/q_o$$

where p_s is static pressure of the flow, and p_{so} , q_o are the pitot static and dynamic pressures. Therefore,

$$C_{ps} = (PT/QO) - (Q/QO) - (PSO/QO)$$

(3) Flow velocity is determined from the measured q and density ρ_s according to

$$V = \sqrt{\frac{2q}{\rho_s}}$$

With the equation of state used to express ρ_s , the above expression becomes

$$V = \sqrt{\frac{2qRT_s}{\rho_s}}$$

where p_s , T_s are the pressure and temperature of the flow, respectively, and R the gas content. The pressure p_s is in turn obtained from

$$p_s = [(PT/QO) - (Q/QO)](QO) + 13.6(\text{PBAR}), \text{ in } H_2O \text{ (abs)}$$

Therefore, the expression for V , assuming $T_s = \text{TPLEN}$, and taking $R = 1716 \text{ ft}^2/\text{s}^2 \cdot \text{R}$, becomes

$$V = 58.58 \sqrt{\frac{(Q/QO)(\text{TPLEN})}{(PT/QO) - (Q/QO) + 13.6(\text{PBAR}/QO)}, \text{ ft/s}}$$

(4) Since the acoustic velocity, c , is

$$c = \sqrt{kRT_s} = \sqrt{kR(TPLEN)}$$

Mach number, $M = V/c$, is computed as

$$M = 1.20 \sqrt{\frac{(Q/QO)}{(PT/QO) - (Q/QO) + 13.6(PBAR/QO)}}$$

in which V from (3) above has been used, and the specific heat ratio, k , taken as 1.4.

(5) Flow velocity components are computed according to V from (3) above and the recorded pitch and corrected yaw angles as

$$V_y = V / \sqrt{1 + \tan^2(YAW) + \tan^2(PITCH)}$$

$$V_x = V_y \tan(YAW)$$

$$V_z = - V_y \tan(PITCH)$$

F4-FO	F5-FO	F1-FO	FO-ATM	YAW	T-BAR	F-BAR	T-FLEN	RO	FOS
-10.334	-9.486	-4.759	9.492	4.51	72.243	29.1	76.277	3.553	M4.12221.25
-10.469	-9.898	-4.335	9.501	4.57	72.098	29.1	76.413	3.553	M4.12224.75
-10.334	-10.036	-4.355	9.483	4.5	72.751	29.1	76.684	3.553	M4.12228.25
-10.385	-10.02	-4.21	9.487	4.15	72.461	29.1	76.616	3.553	M4.12228.75
-10.345	-10.007	-4.277	9.497	4.15	72.824	29.1	76.616	3.553	M4.12229.25
-10.306	-10.04	-4.222	9.477	4.51	73.042	29.1	76.752	3.553	M4.12229.75
-10.309	-10.094	-4.043	9.503	4.51	72.824	29.1	76.684	3.553	M4.122210.25
-10.321	-10.038	-4.201	9.518	4.09	73.405	29.1	77.226	3.553	M4.122210.75
-10.248	-10.033	-4.321	9.51	3.97	73.259	29.1	77.022	3.553	M4.122211.25
-10.237	-10.069	-4.028	9.497	4.63	73.913	29.1	77.497	3.553	M4.122211.75
-10.129	-10.057	-4.247	9.514	4.35	73.913	29.1	77.564	3.553	M4.122212.25
-10.039	-10.111	-4.149	9.531	4.35	73.84	29.1	77.497	3.553	M4.122212.75
-9.949	-10.126	-4.112	9.509	4.63	73.985	29.1	77.767	3.553	M4.122213.25
-9.879	-10.037	-4.351	9.505	4.28	74.493	29.1	77.971	3.553	M4.122213.75
-9.744	-10.048	-4.427	9.496	4.92	74.639	29.1	78.242	3.553	M4.122214.25
-9.653	-9.939	-4.886	9.528	4.91	74.639	29.1	78.309	3.553	M4.122214.75
-9.611	-9.903	-5.265	9.5	4.11	74.856	29.1	78.242	3.553	M4.122214.95
-9.549	-9.859	-5.635	9.524	3.29	74.929	29.1	78.51	3.553	M4.122215.15
-9.558	-9.808	-5.933	9.531	2.61	75.365	29.1	78.783	3.553	M4.122215.35
-9.572	-9.783	-6.121	9.534	1.31	75.51	29.1	78.919	3.553	M4.122215.55
9.575	-9.671	-6.421	9.542	-0.6	75.945	29.1	79.325	3.553	M4.122215.75

FITCH	YAW	Q/RO	FT/RO	RO	VEL	T-BAK	F-BAR	T-FLEN	FOS
-3.690	4.017	1.288	1.331	3.553	129.2	72.243	29.1	535.9	M4.12221.25
-1.796	4.360	1.459	1.452	3.553	129.3	72.098	29.1	536.1	M4.12224.75
-2.756	3.988	1.455	1.441	3.553	129.3	72.751	29.1	536.3	M4.12228.25
-6.063	3.956	1.495	1.483	3.553	129.3	72.461	29.1	536.3	M4.12228.75
-4.850	3.967	1.472	1.467	3.553	129.3	72.824	29.1	536.3	M4.12229.25
-0.058	4.369	1.486	1.477	3.553	129.4	73.042	29.1	536.4	M4.12229.75
2.714	4.401	1.538	1.535	3.553	129.3	72.824	29.1	536.3	M4.122210.25
-1.465	3.940	1.492	1.494	3.553	129.4	73.405	29.1	536.9	M4.122210.75
2.071	3.855	1.453	1.458	3.553	129.4	73.259	29.1	536.7	M4.122211.25
5.071	4.542	1.530	1.537	3.553	129.5	73.913	29.1	537.1	M4.122211.75
9.793	4.305	1.462	1.480	3.553	129.5	73.913	29.1	537.2	M4.122212.25
1.733	4.371	1.484	1.513	3.553	129.5	73.84	29.1	537.1	M4.122212.75
2.271	4.698	1.487	1.517	3.553	129.5	73.985	29.1	537.4	M4.122213.25
2.219	4.343	1.406	1.449	3.553	129.6	74.493	29.1	537.6	M4.122213.75
3.064	5.051	1.376	1.425	3.553	129.6	74.639	29.1	537.9	M4.122214.25
3.148	5.047	1.236	1.305	3.553	129.6	74.639	29.1	537.9	M4.122214.75
3.364	4.263	1.132	1.190	3.553	129.7	74.856	29.1	537.9	M4.122214.95
3.722	3.469	1.027	1.093	3.553	129.7	74.929	29.1	538.2	M4.122215.15
3.417	2.767	0.943	1.011	3.553	129.8	75.365	29.1	538.4	M4.122215.35
3.183	1.450	0.8956	0.997	3.553	129.8	75.51	29.1	538.6	M4.122215.55
2.774	0.0316	0.8036	0.876	3.553	129.9	75.945	29.1	539.0	M4.122215.75

TRAVERSE PLANE 2

SIDEWALL STATIC TAP	STATIC PRESSURE	ENDWALL PROBE POSITION	STATIC PRESSURE
1	.038912273	-4.10	.0201699565
2	-.035796836	-3.00	.0847808533
3	-.054207788	-2.25	.183382956
4	-.065161898	-1.50	.248664211
5	-.078568127	0.00	.387409061
6	-.105521275	1.50	.516039354
7	-.099632182	3.00	.665628268
8	-.107269913	4.10	.706618823
9	-.077261670		
10	-.086547543		
11	-.101501418		
12	-.079794182		
13	-.063915743		
14	-.043514962		
15	-.017466382		
16	.026490865		
17	.6654674098		
18	.7024300054		
19	.7240568398		
20	.7156955376		
21	.7202178765		
22	.7290414632		
23	.7265692512		
24	.7310513946		
25	.7334633097		
26	.7412015364		
27	.730810199		
28	.7269310468		
29	.7213836345		
30	.7123590541		
31	.7104295223		
32	.706369463		

00=3.59144082

FSD/00=0.6189

**DATE
FILMED**

3-8